41. Vielkind, S., Gallagher-Gambarelli, M., Gomez, M., Hinton, H. J., Cantrell, D. A. (2005) Integrin regulation by RhoA in thymocytes. *J. Immunol.* **175**, 350–357.
42. Brenner, B., Koppenhoefer, U., Weinstock, C., Linderkamp, O., Lang, F., Gulbins, E. (1997) Fas- or ceramide-induced apoptosis is mediated by a Rac1-regulated activation of Jun N-terminal kinase/p38 kinases and GADD153. *J. Biol. Chem.* **272**, 22173–22181.
43. Calnan, B. J., Szychowski, S., Chan, F. K., Cado, D., Winoto, A. (1995) A role for the orphan steroid receptor Nur77 in apoptosis accompanying antigen-induced negative selection. *Immunity* **3**, 273–282.
44. Zhou, T., Cheng, J., Yang, P., Wang, Z., Liu, C., Su, X., Bluethmann, H., Mountz, J. D. (1996) Inhibition of Nur77/Nurr1 leads to inefficient clonal deletion of self-reactive T cells. *J. Exp. Med.* **183**, 1879–1892.
45. Szegezdi, E., Kiss, I., Simon, A., Blasko, B., Reichert, U., Michel, S., Sandor, M., Fesus, L., Szondy, Z. (2003) Ligation of retinoic acid receptor α regulates negative selection of thymocytes by inhibiting both DNA binding of nur77 and synthesis of Bim. *J. Immunol.* **170**, 3577–3584.
46. Bouillet, P., Purton, J. F., Godfrey, D. I., Zhang, L. C., Coultas, L., Puthalakath, H., Pellegrini, M., Cory, S., Adams, J. M., Strasser, A. (2002) BH3-only Bcl-2 family member Bim is required for apoptosis of autoreactive thymocytes. *Nature* **415**, 922–926.
47. Weih, F., Ryseck, R. P., Chen, L., Bravo, R. (1996) Apoptosis of nur77/N10-transgenic thymocytes involves the Fas/Fas ligand pathway. *Proc. Natl. Acad. Sci. USA* **93**, 5533–5538.
48. Youn, H. D., Liu, J. O. (2000) Cabin1 represses MEF2-dependent Nur77 expression and T cell apoptosis by controlling association of histone deacetylases and acetylases with MEF2. *Immunity* **13**, 85–94.
49. Dequiedt, F., Kasler, H., Fischle, W., Kiermer, V., Weinstein, M., Herndier, B. G., Verdin, E. (2003) HDAC7, a thymus-specific class II histone deacetylase, regulates Nur77 transcription and TCR-mediated apoptosis. *Immunity* **18**, 687–698.
50. Yang, F. C., Kapur, R., King, A. J., Tao, W., Kim, C., Borneo, J., Breese, R., Marshall, M., Dinauer, M. C., Williams, D. A. (2000) Rac2 stimulates Akt activation affecting BAD/Bcl-XL expression while mediating survival and actin function in primary mast cells. *Immunity* **12**, 557–568.
51. Pekarsky, Y., Hallas, C., Palamarchuk, A., Koval, A., Bullrich, F., Hirata, Y., Bichi, R., Letofsky, J., Croce, C. M. (2001) Akt phosphorylates and regulates the orphan nuclear receptor Nur77. *Proc. Natl. Acad. Sci. USA* **98**, 3690–3694.
52. Masuyama, N., Oishi, K., Mori, Y., Ueno, T., Takahama, Y., Gotoh, Y. (2001) Akt inhibits the orphan nuclear receptor Nur77 and T-cell apoptosis. *J. Biol. Chem.* **276**, 32799–32805.
53. Nakayama, K., Negishi, I., Kuida, K., Shinkai, Y., Louie, M. C., Fields, L. E., Lucas, P. J., Stewart, V., Alt, F. W., et al. (1993) Disappearance of the lymphoid system in Bcl-2 homozygous mutant chimeric mice. *Science* **261**, 1584–1588.
54. Korsmeyer, S. J. (1992) Bcl-2: a repressor of lymphocyte death. *Immunol. Today* **13**, 285–288.
55. Punt, J. A., Suzuki, H., Granger, L. G., Sharrow, S. O., Singer, A. (1996) Lineage commitment in the thymus: only the most differentiated (TCRhibcl-2hi) subset of CD4+CD8+ thymocytes has selectively terminated CD4 or CD8 synthesis. *J. Exp. Med.* **184**, 2091–2099.
56. Catz, S. D., Johnson, J. L. (2001) Transcriptional regulation of bcl-2 by nuclear factor κ B and its significance in prostate cancer. *Oncogene* **20**, 7342–7351.
57. Oukka, M., Ho, I. C., de la Brousse, F. C., Hoey, T., Grusby, M. J., Glimcher, L. H. (1998) The transcription factor NFAT4 is involved in the generation and survival of T cells. *Immunity* **9**, 295–304.
58. Viatour, P., Bentires-Alj, M., Chariot, A., Deregowski, V., de Leval, L., Merville, M. P., Bours, V. (2003) NF-κ B2/p100 induces Bcl-2 expression. *Leukemia* **17**, 1349–1356.
59. Turner, H., Gomez, M., McKenzie, E., Kirchem, A., Lennard, A., Cantrell, D. A. (1998) Rac-1 regulates nuclear factor of activated T cells (NFAT) C1 nuclear translocation in response to Fcε receptor type 1 stimulation of mast cells. *J. Exp. Med.* **188**, 527–537.

Lnk negatively regulates self-renewal of hematopoietic stem cells by modifying thrombopoietin-mediated signal transduction

Jun Seita*†, Hideo Ema*, Jun Ooehara*, Satoshi Yamazaki*‡, Yuko Tadokoro*, Akiko Yamasaki*, Koji Eto*, Satoshi Takaki§, Kiyoshi Takatsu§, and Hiromitsu Nakauchi*¶

*Laboratory of Stem Cell Therapy, Center for Experimental Medicine, and §Division of Immunology, Department of Microbiology and Immunology, Institute of Medical Science, University of Tokyo, 4-6-1 Shirokanedai, Minato-ku, Tokyo 108-8639, Japan; and ‡ReproCell, Inc., Imperial Hotel Tower 12F, 1-1-1 Uchisaiwai-cho, Chiyoda-ku, Tokyo 100-0011, Japan

Edited by Irving L. Weissman, Stanford University School of Medicine, Stanford, CA, and approved December 7, 2006 (received for review July 22, 2006)

One of the central tasks of stem cell biology is to understand the molecular mechanisms that control self-renewal in stem cells. Several cytokines are implicated as crucial regulators of hematopoietic stem cells (HSCs), but little is known about intracellular signaling for HSC self-renewal. To address this issue, we attempted to clarify how self-renewal potential is enhanced in HSCs without the adaptor molecule Lnk, as in Lnk-deficient mice HSCs are expanded in number >10-fold because of their increased self-renewal potential. We show that Lnk negatively regulates self-renewal of HSCs by modifying thrombopoietin (TPO)-mediated signal transduction. Single-cell cultures showed that Lnk-deficient HSCs are hypersensitive to TPO. Competitive repopulation revealed that long-term repopulating activity increases in Lnk-deficient HSCs, but not in WT HSCs, when these cells are cultured in the presence of TPO with or without stem cell factor. Single-cell transplantation of each of the paired daughter cells indicated that a combination of stem cell factor and TPO efficiently induces symmetrical self-renewal division in Lnk-deficient HSCs but not in WT HSCs. Newly developed single-cell immunostaining demonstrated significant enhancement of both p38 MAPK inactivation and STAT5 and Akt activation in Lnk-deficient HSCs after stimulation with TPO. Our results suggest that a balance in positive and negative signals downstream from the TPO signal plays a role in the regulation of the probability of self-renewal in HSCs. In general, likewise, the fate of stem cells may be determined by combinational changes in multiple signal transduction pathways.

c-mpl | p38 MAPK | STAT5 | Akt

Manipulation of stem cell self-renewal is a necessity for the development of stem cell-based regenerative and transplantation medicine. To this end, we need to understand molecular mechanisms underlying self-renewal in stem cells. In hematopoietic stem cells (HSCs), the best-studied mammalian stem cells, self-renewal has been demonstrated by *in vivo* assays (1–4). However, molecular mechanisms regulating self-renewal remain poorly understood. In particular, despite numerous studies of cytokines and cytokine receptors, little is known about intracellular signaling events in self-renewal of HSCs (5–7). Major difficulties have been the paucity of HSCs and the *in vitro* recapitulation of self-renewal (8, 9). We have approached this issue by analyzing Lnk-deficient mice (Lnk−/−) in comparison with WT mice.

Lnk is an adaptor protein containing a proline-rich domain, a pleckstrin homology domain, and a Src homology 2 domain (10). In Lnk−/− mice, long-term marrow repopulating activity is markedly elevated because of increases in both absolute number and self-renewal activity of HSCs (4, 11). These results suggest that Lnk negatively regulates the key signaling pathways of HSC self-renewal. Lnk is expressed in various hematopoietic lineages, in which some of its functions have been reported (12–15). Lnk is thought to regulate stem cell factor (SCF) signaling pathways negatively in immature B cells (12, 13). Recent reports indicated that Lnk negatively regulates thrombopoietin (TPO) signaling in megakaryocytes and erythropoietin signaling in erythroblasts (14, 15). Although the functions of Lnk as a negative regulator of cytokine signaling are shared by these lineages, the target signaling pathways appear to differ among these lineages. We therefore attempted to determine Lnk target signaling pathways in HSCs.

In both WT and Lnk−/− mice, CD34-negative or low, c-Kit-positive, Sca-1-positive, lineage marker-negative ($CD34^-KSL$) cells within adult mouse bone marrow (BM) are highly enriched in HSCs (4, 16). When single-cell transplantation with $CD34^-KSL$ cells was performed, rates of long-term reconstitution were similar in WT and Lnk −/− mice, indicating similar degrees of HSC enrichment in this population. Using these highly enriched HSC populations, we first studied cytokine-induced division of $CD34^-KSL$ cells and found that Lnk is involved in the TPO signaling pathway. We then investigated how HSCs self-renew in culture with TPO by competitive repopulation and paired daughter cell assays. Furthermore, we developed single-cell immunostaining procedures for signal transduction analysis to examine Lnk-interacting intracellular signaling pathways in TPO-stimulated $CD34^-KSL$ cells.

Results

***In Vitro* Survival and Division of Single $CD34^-KSL$ Cells.** Direct effects of cytokines on both survival and proliferation of HSCs were evaluated to see which cytokine signals are influenced by the absence of Lnk. Serum-free culture of single WT or Lnk−/− $CD34^-KSL$ cells was performed in the presence of various cytokines at 100 ng/ml. Every 24 h after initiation of culture, cells in each well were examined under the microscope. At 72 h of culture, no $CD34^-KSL$ cells survived without a cytokine. In contrast, >70% of cells survived in the presence of SCF or TPO, and <20% of cells survived in the presence of IL-3, IL-6, or IL-11 (Fig. 1*A*). When cells were cultured with SCF, frequencies of cell division did not differ between Lnk−/− $CD34^-KSL$ cells (47.9 ± 5.3%) and WT $CD34^-KSL$ cells (54.6 ± 9.1%) (P =

Author contributions: J.S., H.E., and H.N. designed research; J.S., J.O., and A.Y. performed research; J.S., S.Y., Y.T., S.T., K.E., and K.T. contributed new reagents/analytic tools; J.S., H.E., K.E., S.T., and H.N. analyzed data; and J.S., H.E., and H.N. wrote the paper.

The authors declare no conflict of interest.

This article is a PNAS direct submission.

Abbreviations: HSC, hematopoietic stem cell; SCF, stem cell factor; TPO, thrombopoietin; BM, bone marrow; RU, repopulating unit; SCIPhos, single-cell imaging of phosphorylation.

†Present address: Department of Pathology, Stanford University School of Medicine, Stanford, CA 94305.

¶To whom correspondence should be addressed. E-mail: nakauchi@ims.u-tokyo.ac.jp.

This article contains supporting information online at www.pnas.org/cgi/content/full/0606238104/DC1.

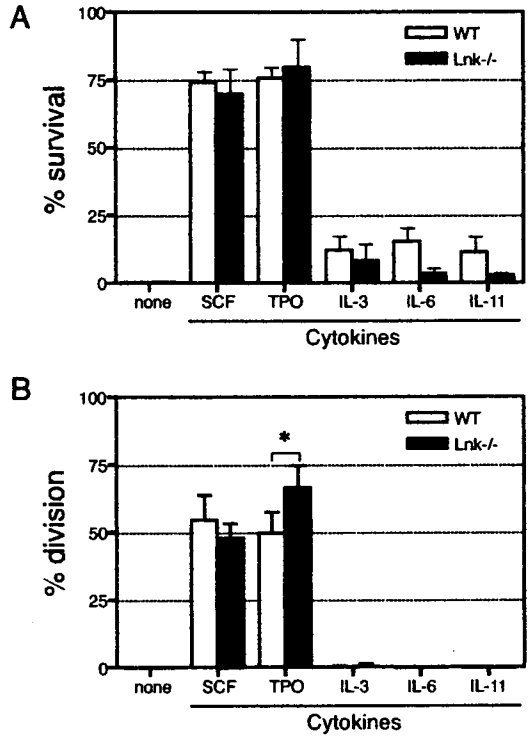

Fig. 1. *In vitro* survival and division of single WT or Lnk−/− CD34⁻KSL cells in the presence of a cytokine. WT or Lnk−/− CD34⁻KSL cells (n = 96) underwent single-cell serum-free culture in the presence of SCF, TPO, IL-3, IL-6, or IL-11. At 72 h of culture, the number of cells in each well was counted under an inverted microscope. Wells containing one or more cell(s) were judged to exhibit "survival" and wells containing two or more cells were judged to exhibit "division." Frequencies of survival (*A*) and division (*B*) from five independent experiments are shown as mean ± SD. *, P = 0.009.

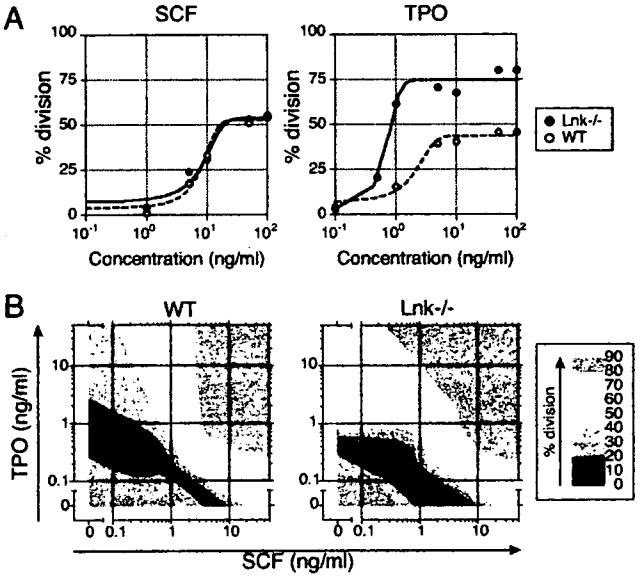

Fig. 2. Hypersensitivity of Lnk−/− CD34⁻KSL cells to TPO stimulation. Dose–response curves to SCF, TPO, or both are shown for WT and Lnk−/− CD34⁻KSL cells. (*A*) (*Left*) When cultured with SCF, WT or Lnk−/− cells had ED_{50}s of 8.03 ± 0.92 or 7.17 ± 2.09 ng/ml, respectively (P = 0.73). (*Right*) When cultured with TPO, WT or Lnk−/− cells had ED_{50}s of 1.89 ± 0.55 or 0.69 ± 0.06 ng/ml, respectively (P = 0.04). (*B*) Synergistic effects of SCF and TPO on division of CD34⁻KSL cells. Percentages of cells having undergone division by 72 h of culture among WT (*Left*) or Lnk−/− (*Right*) CD34⁻KSL cells in the presence of SCF plus TPO are presented as isobolograms. Contours show percent division at intervals of 10%.

0.197). In contrast, when cells were cultured with TPO, the frequency of cell division in Lnk−/− CD34⁻KSL cells (66.7 ± 8.0%) was significantly greater than that in WT CD34⁻KSL cells (49.8 ± 7.6%) (P = 0.009) (Fig. 1*B*). These data indicate that SCF or TPO, but not the other cytokines studied, can support survival and division of significant proportions of WT and Lnk−/− CD34⁻KSL cells, and that TPO promotes division of Lnk−/− CD34⁻KSL cells more efficiently than division of WT CD34⁻KSL cells.

Hypersensitivity of Lnk−/− CD34⁻KSL Cells to TPO Stimulation. Sensitivity to SCF or TPO stimulation was compared between WT and Lnk−/− CD34⁻KSL cells with respect to dose–response of cell division. WT or Lnk−/− CD34⁻KSL cells were subjected to single-cell serum-free culture with graded doses of SCF (1, 5, 10, 50, or 100 ng/ml) or TPO (0.1, 0.5, 1, 5, 10, 50, or 100 ng/ml). After 72 h of culture, frequencies of cell division at each concentration were determined. As shown in Fig. 2*A*, dose–response curves were plotted by nonlinear regression. Midpoint effective doses (ED_{50}s) were obtained for SCF and TPO. When WT or Lnk−/− CD34⁻KSL cells were cultured with SCF, respective ED_{50}s were 8.03 ± 0.92 and 7.17 ± 2.09 ng/ml (P = 0.73). When WT or Lnk−/− cells were cultured with TPO, respective ED_{50}s were 1.89 ± 0.55 and 0.69 ± 0.06 ng/ml (P = 0.04). SCF dose–response behaviors were quite similar in WT and Lnk−/− CD34⁻KSL cells. In contrast, the concentrations of TPO that induced cell division were lower for Lnk−/− CD34⁻KSL cells than for WT CD34⁻KSL cells.

The synergistic effects of SCF and TPO on cell division were compared between WT and Lnk−/− CD34⁻KSL cells. Single-cell serum-free cultures were performed in the presence of SCF and TPO at various combinations of concentrations. At 72 h of culture, frequencies of cell division were determined and demonstrated by isobolography (17, 18) (Fig. 2*B*). When concentrations of both SCF and TPO were >5 ng/ml, > 80% of both WT and Lnk−/− CD34⁻KSL cells underwent cell division. When the concentration of SCF was greater than that of TPO, dose–response behaviors of WT and Lnk−/− CD34⁻KSL cells were similar. In contrast, when the TPO concentration was greater than that of SCF and the SCF concentration was <5 ng/ml, Lnk−/− CD34⁻KSL cells divided more frequently than did WT CD34⁻KSL cells. These results indicate that in CD34⁻KSL cells the absence of Lnk causes hypersensitivity to TPO but not to SCF even when both TPO and SCF are present.

In addition, the kinetics of cytokine-induced cell division was compared between WT and Lnk−/− CD34⁻KSL cells [supporting information (SI) Fig. 5]. When cultured with SCF or SCF and TPO, WT and Lnk−/− CD34⁻KSL cells showed quite similar first-division kinetics. Of note is that the frequencies of cell division were similar in WT and Lnk−/− CD34⁻KSL cells when those cells were cultured with a combination of SCF and TPO at saturating concentrations (Fig. 2*B* and SI Fig. 5). In contrast, when cultured with TPO, it became apparent after 24 h of culture that Lnk−/− CD34⁻KSL cells underwent a first division more frequently than did WT CD34⁻KSL cells (SI Fig. 5).

Repopulating Activity Increases in Lnk−/− CD34⁻KSL Cells in Response to TPO. We assumed that TPO might be able to induce self-renewal in Lnk−/− HSCs more efficiently than in WT HSCs. To address this issue, 40 WT or Lnk−/− CD34⁻KSL cells were cultured in serum-free medium in the presence of cytokines for 72 h and underwent competitive repopulation assay (SI Fig. 6*A*). Twelve weeks after transplantation, repopulating units

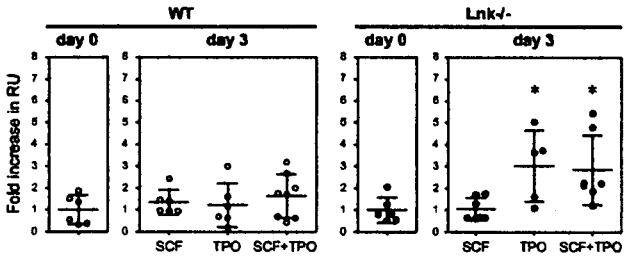

Fig. 3. RU increase in Lnk−/− CD34⁻KSL cells after culture. Forty WT (*Left*) or Lnk−/− (*Right*) CD34⁻KSL cells were transplanted (n = 8). Similar cells alternatively were cultured with SCF (50 ng/ml) and/or TPO (50 ng/ml) for 3 days, and then transplanted (n = 8). RUs before (n = 8) and after culture were compared 12 weeks after transplantation. Data are shown in terms of fold increase (average RU before culture = 1.0). RUs significantly increased in Lnk−/− CD34⁻KSL cells after culture with TPO (P = 0.025) or SCF plus TPO (P = 0.046). *, $P < 0.05$ vs. before culture.

(RUs) were determined by analyzing peripheral blood donor chimerism. The RU is a quantitative index of repopulating activity, and 1 RU is defined as the amount of repopulating activity in 10^5 unfractionated BM cells from WT mice, based on competitive repopulation assay (19).

As shown in Fig. 3, RUs did not change in WT CD34⁻KSL cells after a 72-h culture period in the presence of SCF, TPO, or SCF plus TPO. RUs did not change significantly in Lnk−/− CD34⁻KSL cells after culture with SCF alone. However, RUs were significantly increased in Lnk−/− CD34⁻KSL cells after culture with TPO alone or SCF plus TPO. These repopulating activities were transplantable into secondary recipient mice (SI Table 2), suggesting that self-renewal potential was maintained in cultured cells. On average, RU increased 3-fold in both cases. Based on the positive correlation between RUs and HSC numbers (SI Fig. 6*B*), it was estimated that the number of HSCs proportionately increased 3-fold. To increase in number, HSCs should have undergone symmetrical self-renewal divisions.

Symmetrical Self-Renewal Division of Lnk−/− HSCs in Culture. To know whether increased RUs in effect resulted from symmetrical self-renewal in Lnk−/− HSCs, paired daughter cell experiments were performed (SI Fig. 6*C*). Single CD34⁻KSL cells were directly transplanted into lethally irradiated mice or individually cultured in the presence of SCF and TPO. When cells in culture gave rise to two daughter cells, each daughter cell was separated from the other by micromanipulation techniques. Individual daughter cells were transplanted into lethally irradiated mice.

As shown in Table 1, both daughter cells were detected as long-term repopulating cells in 3 of 20 pairs of daughters of single Lnk−/− CD34⁻KSL cells and in none of 28 pairs of daughters of single WT CD34⁻KSL cells. One of the two daughter cells was detected as a long-term repopulating cell in 3 of 20 pairs of daughters of Lnk−/− CD34⁻KSL cells and in 3 of 28 pairs of daughters of WT CD34⁻KSL cells. When symmetrical self-renewal is defined as division resulting in generation of two daughter cells with long-term repopulation potential, and asymmetrical self-renewal is defined as division resulting in generation of one daughter cell with long-term repopulating potential and another without long-term repopulation potential, these data support the conclusion that in culture with SCF and TPO, Lnk−/− HSCs undergo symmetrical self-renewal division more frequently than do WT HSCs.

Development of Signal Transduction Analysis for HSCs. Because of the paucity of HSCs (a single mouse yielded ≈1,000 CD34⁻KSL cells) to apply commonly used signal transduction assays to this study was difficult. To circumvent this problem, we combined multicolor fluorescence-activated cell sorting, fluorescent immunostaining, confocal laser scanning, and computational quantification of fluorescent intensities. One of the two keys to success in this assay was in-droplet immunostaining procedures. Their principal steps are illustrated in SI Fig. 7. From the initial cell purification step to the final analysis step, cells were maintained in a droplet of medium to avoid cell loss and cell damage. The other key was measurement of signal intensity in individual cells. In this study, we focused on phosphorylation kinetics of signaling molecules because Lnk is an adaptor protein containing a Src homology 2 domain. As demonstrated in SI Fig. 8, phosphorylation intensity of each CD34⁻KSL cell was evaluated by using NIH ImageJ software. We named this method the single-cell imaging of phosphorylation (SCIPhos) assay.

To validate the SCIPhos assay, signal transduction in a cytokine-dependent cell line was examined simultaneously by both SCIPhos assays and conventional Western blot analysis. After cytokine deprivation, TPO-dependent 32D/Mpl cells were stimulated with TPO, and phosphorylation of STAT5 and Jak2 was quantitatively measured. As representatively shown in SI Fig. 9, SCIPhos and Western blot analyses gave similar kinetics of STAT5 phosphorylation. Interestingly, STAT5 phosphorylation increased in a dose-dependent manner for TPO stimulation, and SCIPhos data correlated well with Western blot data (SI Fig. 9*C*). Good correlation between results of these two assay techniques was also observed for Jak2 phosphorylation (data not shown).

Phosphorylation of Signaling Molecules in WT and Lnk−/− CD34⁻KSL Cells. To identify the key signal pathways involved in HSC self-renewal, phosphorylation kinetics of JAK2, STAT3, STAT5, Akt, p38 MAPK, and p44/42 MAPK after TPO or SCF stimulation was compared between WT and Lnk−/− CD34⁻KSL

Table 1. Symmetrical self-renewal in culture of Lnk −/− CD34⁻ KSL cells but not WT CD34⁻ KSL cells

Single CD34⁻ KSL cells	Daughter cells: One	Daughter cells: The other	No. of pairs (%)	% Chimerism
WT	+	+	0/28 (0)	
WT	+	−	3/28 (11)	0.6, 0.6, 0.6
Lnk−/−	+	+	3/20 (15)	(2.0; 5.9), (50.9; 72.9), (42.9; 81.4)
Lnk−/−	+	−	3/20 (15)	0.7, 2.4, 23.0

Single WT or Lnk−/− CD34⁻KSL cells were cultured with SCF and TPO. After a single cell gave rise to paired-daughter cells, each daughter cell was individually transplanted (SI Fig. 6C). Twelve weeks after transplantation reconstitution was observed in 4 of 25 mice or 3 of 16 mice that, respectively, had received single WT or Lnk−/− CD34⁻KSL cells at day 0. Successful reconstitution is shown as +, and undetectable reconstitution is shown as −, for each transplanted daughter cell.

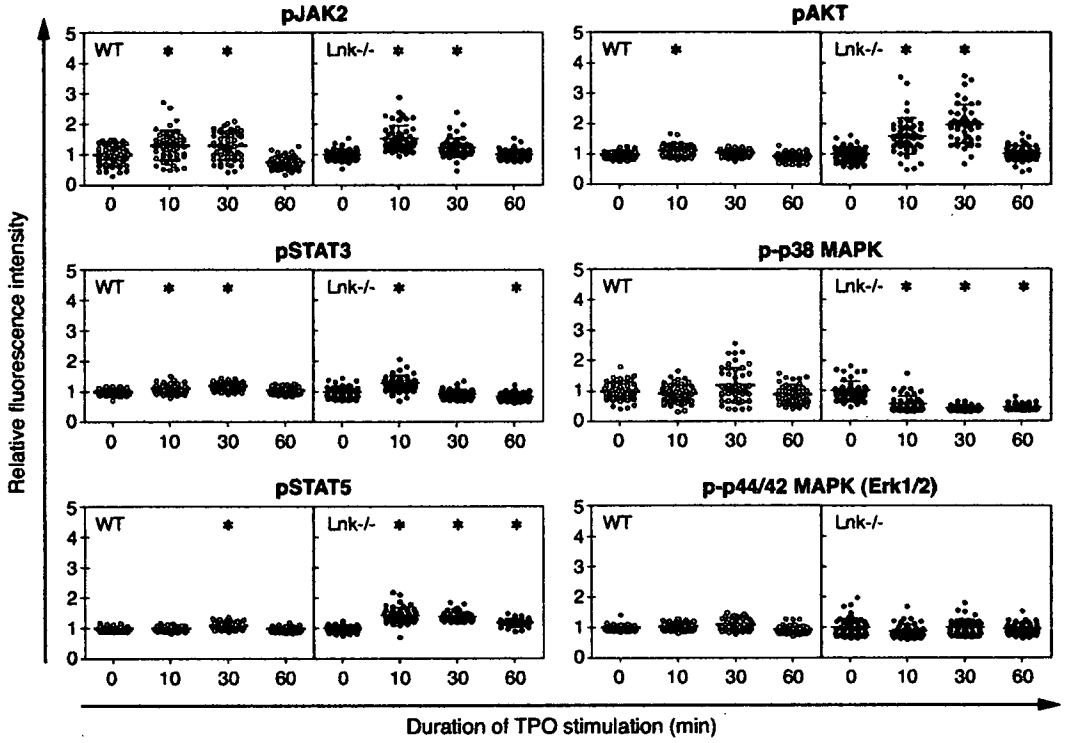

Fig. 4. TPO-mediated signal transduction in WT and Lnk−/− CD34⁻KSL cells. Phosphorylation kinetics of JAK2, STAT3, STAT5, Akt, p38 MAPK, and p44/42 MAPK in TPO-stimulated WT and Lnk−/− CD34⁻KSL cells. All fluorescence intensities of individual cells were computationally quantified, normalized, and compared against the mean intensity of unstimulated cells. Each dot shows normalized fluorescence intensity of individual cells (n = 50). Error bars indicate mean ± SD. *, $P < 0.001$ vs. unstimulated cells (t = 0).

cells. As shown in Fig. 4, after stimulation with TPO JAK2 was similarly phosphorylated in WT and Lnk−/− CD34⁻KSL cells. However, STAT5 and Akt were more intensely phosphorylated in Lnk−/− CD34⁻KSL cells than in WT CD34⁻KSL cells. In contrast, phosphorylation levels of p38 MAPK in Lnk−/− CD34⁻KSL cells were down-regulated after TPO stimulation, whereas those in WT CD34⁻KSL cells remained unchanged. Significant phosphorylation of p44/42 MAPK was not detected in either cell type. On the other hand, after stimulation with SCF, we detected no significant difference between WT and Lnk−/− CD34⁻KSL cells in phosphorylation patterns of these signaling molecules (data not shown). Because these comparisons were made with actively self-renewing HSCs, enhanced up-regulation of STAT5 and Akt pathways and enhanced down-regulation of p38 MAPK pathways can be inferred to be associated with initiation of HSC self-renewal.

Discussion

To understand why self-renewal potential is greater in HSCs without Lnk, we focused our attention on a first division of CD34⁻KSL cells because self-renewal is likely to be progressively reduced in the following divisions (7, 8). Analysis of their first division revealed that Lnk−/− CD34⁻KSL cells are more sensitive to TPO than are WT CD34⁻KSL cells. SCF and TPO synergistically acted on both WT and Lnk−/− CD34⁻KSL cells and efficiently induced their division. Over 80% of both WT and Lnk−/− CD34⁻KSL cells divided once by day 3 of culture in the presence of saturating amounts of SCF and TPO (Fig. 2 and SI Fig. 5). Finding that the frequency of dividing cells among Lnk−/− CD34⁻KSL cells did not differ from that among WT CD34⁻KSL cells led us to the hypothesis that outcomes of a first division might differ between WT and Lnk−/− CD34⁻KSL cells. This hypothesis was supported by competitive repopulation data and was verified by paired-daughter cell experiment data. During 3-day culture with TPO or with SCF and TPO, RUs increased 3-fold in Lnk−/− cells, whereas RUs did not significantly increase in WT cells (Fig. 3*A*). To increase RUs, Lnk−/− CD34⁻KSL cells must have undergone symmetrical self-renewal division during the culture period. As far as first divisions were examined, both symmetrical and asymmetrical self-renewal divisions were detected in Lnk−/− CD34⁻KSL cells (Table 1). In contrast, symmetrical self-renewal division was not detected in WT CD34⁻KSL cells. The results clearly indicate that Lnk−/− HSCs self-renew better than do WT HSCs in response to TPO.

Nolan and colleagues (20–22) have reported an intracellular phospho-protein analysis technique using flow cytometry (Phospho Flow). This technique enables signal transduction analysis of target cells in heterogeneous cell populations. The cells that surround CD34-KSL cells, however, have produced many cytokines before a particular experimental stimulus is applied to CD34-KSL cells. The unavoidable prestimulatory effects of these cytokines impair the utility of the Phospho Flow method in the analysis of CD34⁻KSL cells. Furthermore, internalization of c-Kit in response to SCF makes phenotypic identification of CD34-KSL cells difficult. To overcome these problems, in the SCIPhos assay cells are first sorted and then stimulated with cytokines under defined conditions, followed by single-cell immunostaining. The SCIPhos assay enables quantitative measurement of phosphorylation levels of signal transduction molecules in individual cells, as verified by comparison with Western blotting data using only 50 cells (SI Fig. 5). Moreover, intracellular localization of signal molecules can be examined simultaneously (23).

Using SCIPhos assays, we attempted to identify signal transduction pathways that in self-renewing Lnk−/− HSCs are activated or inactivated differently from those in self-renewing

WT HSCs. Because RUs in cultured Lnk−/− cells increased in the presence of TPO alone, but not SCF alone, to the same extent as that seen in the presence of SCF plus TPO (Fig. 3), we simply compared SCF- or TPO-mediated signal transduction between Lnk−/− and WT HSCs. Lnk−/− HSCs in the process of self-renewal revealed enhancement of combinatorial change in signal transduction, i.e., activation of both STAT5 and Akt signal transduction and inactivation of p38 MAPK (Fig. 4). Phoshorylation of p38 MAPK in freshly isolated HSCs was possibly caused by stress in cell preparation procedures. However, its dephosphorylation was significantly enhanced in Lnk−/− HSCs. Kato *et al.* (24) have recently reported that continuous activation of STAT5, but not STAT3, in $CD34^-KSL$ cells results in myeloproliferative disease accompanied with increase of a broad range of myeloid progenitors in addition to HSCs. Akt has been shown to facilitate cell cycle progression and suppression of apoptosis (25). The p38 MAPK pathway has been implicated as regulating cell cycle progression negatively by activating transcription of the Ink4a-Arf locus and inhibiting the expression of D-type cyclins (26). A p38 MAPK inhibitor reportedly prevents decline of self-renewal potential in HSCs through serial transplantation (27). These signal modifications together may give HSCs advantages in maintaining self-renewal potential. How Lnk controls the probability of symmetrical self-renewal in HSCs is extremely intriguing.

No hematopoietic malignancy has been observed to date in Lnk-deficient mice (11, 28). Lnk may provide a suitable molecular target for enhancement of self-renewal capacity of HSCs. Lnk inhibitors should give selective advantage to HSCs and should be useful for stem cell transplantation or gene therapy targeting HSCs. Alternatively, Lnk inhibitors can be used for *ex vivo* expansion of HSCs. Takizawa *et al.* (29) have reported that transient inhibition of endogenous Lnk activity by introduction of a dominant-negative form of Lnk can increase engraftment rates of HSCs. Interestingly, inhibition of Lnk function increases cell adhesion ability in HSCs so that HSCs can efficiently home to a BM niche. These results suggest that Lnk interacts with multiple signaling cascades related to cytokine signal transduction and cell mobility.

In this study, we showed that Lnk negatively regulates TPO-mediated signaling pathways in HSCs. Comparison of HSC numbers among Lnk−/−, TPO−/−, and Lnk−/−TPO−/− mice has recently been reported (28). Increases in numbers of HSCs in Lnk−/− mice have been shown to be overridden by decreases in numbers of HSCs in TPO−/− mice (28). Interestingly, HSC numbers are greater in Lnk−/−TPO−/− mice than in TPO−/− mice, suggesting that not only TPO signaling is involved. We conclude that Lnk negatively interacts with signaling pathways downstream of TPO/c-Mpl that play an important role in HSC fate decision, namely, whether or not HSCs self-renew. We finally propose that self-renewal of HSC is regulated by a balance in positive and negative signals from multiple pathways rather than by self-renewal-specific signals. In this regard, self-renewal signaling may be much more complicated than generally thought.

Materials and Methods

Mice. C57BL/6 mice congenic for the Ly5 locus (B6-Ly5.1) and Lnk−/− B6-Ly5.1 mice were bred and maintained at the Animal Research Center of the Institute of Medical Science, University of Tokyo. The Animal Experiment Committee of the Institute of Medical Science, University of Tokyo, approved animal care and use. B6-Ly5.1/5.2 (B6-F1) mice were obtained from mating pairs of B6-Ly5.1 and B6-Ly5.2 mice. B6-Ly5.2 mice were purchased from Nihon SLC (Shizuoka, Japan).

Purification of $CD34^-KSL$ Cells. $CD34^-KSL$ cells were purified from BM cells of 2-month-old WT or Lnk−/− B6-Ly5.1 mice as described (16, 30). In brief, low-density cells were isolated on Ficoll-Paque PLUS (Amersham Bioscience, Uppsala, Sweden). The cells were stained with an antibody mixture consisting of biotinylated anti-Gr-1, anti-Mac-1, anit-B220, anti-CD4, anti-CD8, and anti-Ter-119 antibodies (Pharmingen, San Diego, CA). The cells were subsequently labeled with MACS goat anti-rat IgG microbeads. Lineage-positive cells were then depleted by using the Midi-MACS system (Miltenyi Biotec, Bergisch Gladbach, Germany). The cells were further stained with FITC-conjugated anti-CD34, phycoerythrin-conjugated anti-Sca-1, and allophycocyanin (APC)-conjugated anti-c-Kit antibodies (Pharmingen). Biotinylated antibodies were detected with streptavidin-APC-Cy7 (Molecular Probes, Eugene, OR). Four-color analysis and sorting were performed on a MoFlo Cell Sorter (DakoCytomation, Glostrup, Denmark).

Single-Cell Serum-Free Culture. Single-cell cultures of $CD34^-KSL$ cells were performed under serum-free conditions as described (9, 31). Cells were individually deposited into single wells of a 96-well round-bottom microtiter plate and cultured in S-clone SF-O3 medium (Sanko-Junyaku, Tokyo, Japan) supplemented with 0.5% BSA and the following cytokines: 0.1–100 ng/ml mouse SCF, 0.1–100 ng/ml human TPO, 100 ng/ml mouse IL-3, 100 ng/ml human IL-6, and 100 ng/ml human IL-11 (PeproTech, Rocky Hill, NJ). After cell sorting, the presence of one cell per well was verified under an inverted microscope. The cells were incubated at 37°C in a humidified atmosphere with 5% CO_2 in air. At several time points, numbers of cells per well were counted under an inverted microscope. Each frequency of cell division was obtained from 96 wells.

Transplantation Assays. Competitive repopulation assays were performed with the Ly5 congenic mouse system. Forty $CD34^-KSL$ cells from WT B6-Ly5.1 mice were transplanted into a WT B6-Ly5.2 mouse irradiated at a dose of 9.5 Gy with 4×10^5 competitor cells from WT B6-F1 mice. Forty $CD34^-KSL$ cells from Lnk−/− B6-Ly5.1 mice were transplanted into a WT B6-Ly5.2 mouse irradiated at a dose of 9.5 Gy with 8×10^5 competitor cells from WT B6-F1 mice. Concurrently, 40 WT or Lnk−/− $CD34^-KSL$ cells were cultured in the presence of cytokines for 3 days, and then transplanted, with 4×10^5 or 8×10^5 WT B6-F1 competitor cells, respectively, into a lethally irradiated (9.5 Gy) WT B6 mouse. When one $CD34^-KSL$ cell or each one of its paired-daughter cells generated in culture was transplanted, 2×10^5 competitor cells were used. Twelve weeks after transplantation, peripheral blood cells of the recipients were stained with FITC-conjugated anti-Ly5.2 (104) and biotinylated anti-Ly5.1 (A4) (Pharmingen). The cells were simultaneously stained with phycoerythrin (PE)-Cy7-conjugated anti-B220 antibody and a mixture of allophycocyanin-conjugated anti-Mac-1 and -Gr-1 antibodies and a mixture of PE-conjugated anti-CD4 and -CD8 antibodies (Pharmingen). The biotinylated antibody was detected with streptavidin-Texas red. Cells were analyzed on a FACS Vantage (Becton Dickinson, San Jose, CA). Percentage chimerism was calculated as (percent Ly5.1-donor cells) × 100/(percentage Ly5.1-donor cells + percentage F1-competitor cells). RUs were calculated with Harrison's method (19) as follows: RU = (percentage chimerism) × (number of competitor cells) × 10^{-5}/(100 − percentage chimerism). In the case of single-cell transplantation, when percentage chimerism was >0.5, test donor cells were considered to be long-term repopulating cells. Secondary transplantation was performed 4 months after primary transplantation. After peripheral blood was analyzed for chimerism once again, 2×10^6 BM cells from selected recipient mice were transplanted into mice irradiated at a dose of 9.5 Gy.

Cell Lines. 32D cells (ATCC, Manassas, VA) were maintained in RPMI medium 1640 with 10% FCS and 10% conditioned

medium from the culture of WEHI-3B cells. Human *c-MPL* cDNA was ligated to the pMY-IRES-EGFP retroviral vector (a gift of T. Kitamura, University of Tokyo, Tokyo, Japan). The recombinant viruses were produced by transfecting pMY-Mpl-IRES-EGFP into 293gp cells with pcDNA3-VSV-G. 32D cells were then infected with these viruses. TPO-dependent 32D (32D/Mpl) cells were selected, cloned, and maintained with 10 ng/ml TPO.

SCIPhos Assay. Phosphorylation of cytokine signaling molecules was analyzed by fluorescent immunocytostaining (SI Fig. 7). WT or Lnk−/− $CD34^{-}KSL$ cells were directly sorted by flow cytometry into droplets of medium on poly-L-lysine-coated glass slides (Matsunami Glass, Osaka, Japan). Cells were stimulated with cytokine(s) at indicated concentrations for indicated times, and then fixed with 4% paraformaldehyde and permeabilized with 0.1% Triton X-100. Subsequently, the cells were stained with phosphorylation-specific anti-JAK2 (Tyr-1007/1008), anti-STAT3 (Tyr-705), anti-STAT5 (Tyr-694), anti-Akt (Ser-473), anti-p38 MAPK (Thr-180/Tyr-182), and anti-p44/42 MAPK (Thr-202/Tyr-204) antibodies (Cell Signaling Technology, Beverly, MA). After washing with PBS containing 2% goat serum, cells were stained with Alexa Fluor 488- or 647-conjugated goat anti-rabbit IgG antibody (Molecular Probes) and DAPI.

To avoid quenching of fluorescence, cells were scanned only once, at the cells' centers, by a TCS SP2 AOBS confocal laser-scanning microscope (Leica, Wetzlar, Germany). Cell images were obtained at 100 × 100 pixels resolution by using a ×63 objective lens. Fluorescence intensities of individual cells (n = 50) were computationally quantified by using ImageJ 1.33 software (http://rsb.info.nih.gov/ij) and were normalized against the mean intensity of unstimulated cells.

Western Blot Analysis. 32D/Mpl cells were starved in RPMI medium 1640 with 10% FCS for 12 h. A total of 2×10^5 such cells were stimulated with 50 ng/ml TPO for 0, 1, 5, 10, or 60 min or 0, 0.8, 1.6, 3.2, 6.4, or 12.8 ng/ml TPO for 10 min. Cells were lysed in buffer consisting of 50 mM Tris·HCl, 5 mM EDTA, 150 mM NaCl, 1% Triton X-100, 1 mM Na_3VO_4, 1 mM NaF, and protease inhibitor in water (Roche Molecular Biochemicals, Basel, Switzerland). Cell lysates in 2× SDS sample buffer (BioRad Laboratories, Hercules, CA) were subjected to SDS/PAGE, blotted, and probed with antiphosphorylated STAT5 (Tyr-694) or antiphosphorylated JAK2 (Tyr-1007/1008) antibodies. Primary antibodies were detected with the SuperSignal West Pico system (Pierce Biotechnology, Rockford, IL).

Statistical Analysis and Nonlinear Regression. Mean values of two groups were compared by two-tail unpaired t testing. Nonlinear regression by the four-parameter logistic method was performed for the dose–response and division kinetics curves. The ED_{50}s of the two groups were compared by F testing. All statistical analyses were performed on Prism 4 software (GraphPad, San Diego, CA).

We thank T. Kitamura for providing human *c-MPL* cDNA and pMY-IRES-EGFP retroviral vector, A. S. Knisely for critical reading of the manuscript, A. Iwama for helpful discussions, and Y. Yamazaki for excellent assistance in analysis and sorting on a flow cytometer. This work was supported in part by grants from the Naito Foundation, the Terumo Lifescience Foundation, and the Ministry of Education, Culture, Sport, Science, and Technology of Japan.

1. Dick JE, Magli MC, Huszar D, Phillips RA, Bernstein A (1985) *Cell* 42:71–79.
2. Lemischka IR, Raulet DH, Mulligan RC (1986) *Cell* 45:917–927.
3. Keller G, Snodgrass R (1990) *J Exp Med* 171:1407–1418.
4. Ema H, Sudo K, Seita J, Matsubara A, Morita Y, Osawa M, Takatsu K, Takaki S, Nakauchi H (2005) *Dev Cell* 8:907–914.
5. Ogawa M (1993) *Blood* 81:2844–2853.
6. Eaves C, Miller C, Conneally E, Audet J, Oostendorp R, Cashman J, Zandstra P, Rose-John S, Piret J, Eaves A (1999) *Ann NY Acad Sci* 872:1–8.
7. Nakauchi H, Sudo K, Ema H (2001) *Ann NY Acad Sci* 938:18–24; discussion 24–25.
8. Ema H, Takano H, Sudo K, Nakauchi H (2000) *J Exp Med* 192:1281–1288.
9. Takano H, Ema H, Sudo K, Nakauchi H (2004) *J Exp Med* 199:295–302.
10. Takaki S, Watts JD, Forbush KA, Nguyen NT, Hayashi J, Alberola-Ila J, Aebersold R, Perlmutter RM (1997) *J Biol Chem* 272:14562–14570.
11. Takaki S, Morita H, Tezuka Y, Takatsu K (2002) *J Exp Med* 195:151–160.
12. Takaki S, Sauer K, Iritani BM, Chien S, Ebihara Y, Tsuji K, Takatsu K, Perlmutter RM (2000) *Immunity* 13:599–609.
13. Velazquez L, Cheng AM, Fleming HE, Furlonger C, Vesely S, Bernstein A, Paige CJ, Pawson T (2002) *J Exp Med* 195:1599–1611.
14. Tong W, Lodish HF (2004) *J Exp Med* 200:569–580.
15. Tong W, Zhang J, Lodish HF (2005) *Blood* 105:4604–4612.
16. Osawa M, Hanada K-i, Hamada H, Nakauchi H (1996) *Science* 273:242–245.
17. Gessner PK (1995) *Toxicology* 105:161–179.
18. Tallarida RJ (2001) *J Pharmacol Exp Ther* 298:865–872.
19. Harrison DE, Jordan CT, Zhong RK, Astle CM (1993) *Exp Hematol* 21: 206–219.
20. Krutzik PO, Nolan GP (2003) *Cytometry A* 55:61–70.
21. Krutzik PO, Hale MB, Nolan GP (2005) *J Immunol* 175:2366–2373.
22. Perez OD, Nolan GP (2002) *Nat Biotechnol* 20:155–162.
23. Yamazaki S, Iwama A, Takayanagi S, Morita Y, Eto K, Ema H, Nakauchi H (2006) *EMBO J* 25:3515–3523.
24. Kato Y, Iwama A, Tadokoro Y, Shimoda K, Minoguchi M, Akira S, Tanaka M, Miyajima A, Kitamura T, Nakauchi H (2005) *J Exp Med* 202:169–179.
25. Alvarez B, Martinez AC, Burgering BM, Carrera AC (2001) *Nature* 413: 744–747.
26. Bulavin DV, Phillips C, Nannenga B, Timofeev O, Donehower LA, Anderson CW, Appella E, Fornace AJ, Jr (2004) *Nat Genet* 36:343–350.
27. Ito K, Hirao A, Arai F, Takubo K, Matsuoka S, Miyamoto K, Ohmura M, Naka K, Hosokawa K, Ikeda Y, Suda T (2006) *Nat Med* 12:446–451.
28. Buza-Vidas N, Antonchuk J, Qian H, Mansson R, Luc S, Zandi S, Anderson K, Takaki S, Nygren JM, Jensen CT, Jacobsen SE (2006) *Genes Dev* 20: 2018–2023.
29. Takizawa H, Kubo-Akashi C, Nobuhisa I, Kwon SM, Iseki M, Taga T, Takatsu K, Takaki S (2006) *Blood* 107:2968–2975.
30. Sudo K, Ema H, Morita Y, Nakauchi H (2000) *J Exp Med* 192:1273–1280.
31. Iwama A, Oguro H, Negishi M, Kato Y, Morita Y, Tsukui H, Ema H, Kamijo T, Katoh-Fukui Y, Koseki H, *et al.* (2004) *Immunity* 21:843–851.

Mini Review

Transient blocking of Lnk-mediated pathways as a potential approach to promote engrafting ability of hematopoietic progenitor cells

Hitoshi Takizawa[1], Kiyoshi Takatsu[1] and Satoshi Takaki[1,2,*]

[1]Division of Immunology, Department of Microbiology and Immunology, The Institute of Medical Science, University of Tokyo, Tokyo, Japan

[2]Department of Community Health and Medicine, Research Institute International Medicine of Japan, Tokyo, Japan

Lnk, an intracellular adaptor protein functions as a negative regulator of B lymphopoiesis, megakaryopoiesis and erythropoiesis by modulating signals through c-Kit, c-Mpl and Epo-R, respectively. In recent studies, we and other groups have shown that *Lnk-/-* mice display an increased number and enhanced repopulating capability of hematopoietic stem or progenitor cells (HSC/Ps), which is due to their hyperresponsiveness to thrombopoietin. Moreover, we have demonstrated that Src homology-2 (SH2) domain of Lnk is essential for the inhibitory function and that Lnk mutants with a point mutation in the SH2 domain potently act as dominant-negative mutant (DN-Lnk). Forced expression of DN-Lnk in HSC/Ps enhanced their repopulating capability in lethally irradiated recipient mice. Remarkably, transient expression of DN-Lnk also facilitated engraftment of HSC/Ps in immunodeficient animal under nonmyeloablative condition, leading to full reconstitution of lymphoid lineage cells. Transwell migration assay revealed that an interaction between HSC/Ps and vascular cell adhesion molecule-1 (VCAM-1) was augmented by Lnk deficiency or expression of DN-Lnk. These results suggest that Lnk modulates cell mobility of HSC/Ps in addition to their expansion. Lnk-mediated pathway therefore could become a potential target for enhancing both integrin-mediated engraftment and cytokine-dependent expansion of HSC/Ps.

Rec.10/10/2006, Acc.11/17/2006, pp59-64

* Correspondence should be addressed to:
Satoshi Takaki, Department of Community Health and Medicine, Research Institute International Medicine of Japan, 1-21-1 Toyama, Shinjuku-ku, Tokyo 162-8655, Japan. Phone: +81-3-3202-7181, Fax: +81-3-3208-5421, e-mail: stakaki@ri.imcj.go.jp

Key words adaptor protein, dominant-negative, hematopoietic stem cells, gene therapy, bone marrow transplantation

Introduction

Hematopoietic stem cells (HSCs) have the self-renewal activity and give rise to all lineages of blood system throughout the lifetime of an individual. The unique biological properties of HSCs have already been utilized extensively for therapeutic strategy to cure hematologic malignancies or genetic diseases by bone

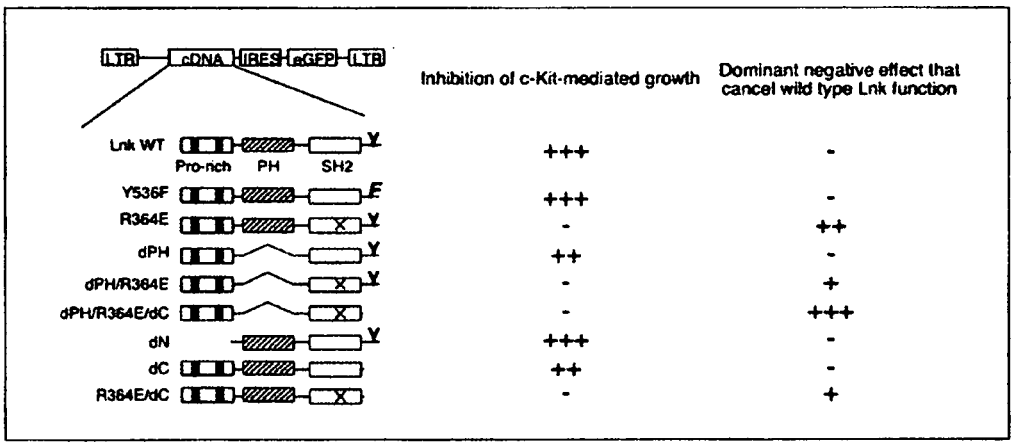

Fig.1 Functional domains of Lnk in c-Kit-mediated cell growth and screening of dominant-negative Lnk mutants

(Left column) Schematic representation of retroviral vector includes IRES between cDNA encoding Lnk mutants and eGFP. (Middle column) Effect of indicated Lnk mutants on c-Kit-mediated growth of MC9 cells. (Right column) Dominant negative effect of indicated Lnk mutants on c-Kit-mediated growth inhibition of MC9 transfectant overexpressing Lnk (MC9-Lnk).

marrow transplantation for decades. However, since the number of available HSCs is limited (e.g. cord blood trans-plantation), *ex vivo* or *in vivo* expansion of HSC by genetic manipulation has been studied intensively[1].

Lnk, together with APS (adaptor molecule containing PH and SH2 domains) and SH2-B, forms an adaptor protein family whose members share a N-terminal homologous domain followed by pleckstrin homology (PH) domain, SH2 domain and a highly conserved tyrosine phosphorylation site at a C-terminus. Because of their structural similarity, nomenclature of this family genes has been recently approved by the HUGO Gene Nomenclature Committee as SH2B adaptor protein 1 (SH2B1) for SH2-B, SH2B2 for APS and SH2B3 for Lnk. Lnk is an intracellular adaptor protein mainly expressed on lymphocyte, megakaryocyte and hematopoietic stem or progenitor cells (HSC/Ps)[2,3]. In previous reports, we and others have demonstrated that *Lnk*-deficient mice show overproduction of lymphocytes and megakaryocytes due to augmentation of growth signals through c-Kit and c-Mpl, respectively[2-4]. In addition, the mice show increased number and enhanced repopulating ability of HSC/Ps, which are caused by their hypersensitivity to thrombopoietin (TPO) in the absence of Lnk[2,3,5]. Despite of these phenotypes, any obvious tumor formations have not been observed in *Lnk*-deficient mice on C57BL6/J background. Inhibition of Lnk-mediated pathway(s) therefore could be a potentially useful approach for *in vivo* or *in vitro* amplification of HSC/Ps without causing malignant transformation.

This mini-review focuses on establishment of a new approach to enhance the engrafting ability of HSC/Ps by blocking Lnk-mediated pathways. First, we identified functional domain of Lnk and generated dominant-negative Lnk mutant (DN-Lnk) that potently inhibits endogenous Lnk function. Second, we showed the effectiveness of DN-Lnk expression on multilineage reconstitution by HSC/Ps after transplantation and its efficacy for treatment of immunodeficient mice. Lastly, we will discuss the regulatory mechanism underlying the high repopulating ability of *Lnk*-deficient HSC/Ps.

Functional domains of Lnk in c-Kit-mediated proliferation

To determine the functional domains of Lnk, various Lnk mutants were constructed and influence of these mutants to c-Kit mediated cell growth was studied (Fig.1). Mast cell line MC9 were retrovirally transduced with Lnk mutants and then c-Kit-mediated growth of transduced cells was compared with that of non-transduced. MC9 cells expressing wild-type Lnk failed to proliferate, suggesting efficient inhibition of c-Kit-mediated cell growth by Lnk. Either deletion of N-terminal domain (dN) or mutation of a conserved tyrosine phosphorylation site (Y536F) showed a similar inhibitory effect compared to wild-type Lnk, while deletion of PH domain (dPH) or C-terminal tail (dC) partly reduced the inhibitory effect. Importantly, a point mutation in SH2 domain (R364E) completely abolished the growth inhibition (Fig.1). These results indicate that SH2 domain of Lnk has a

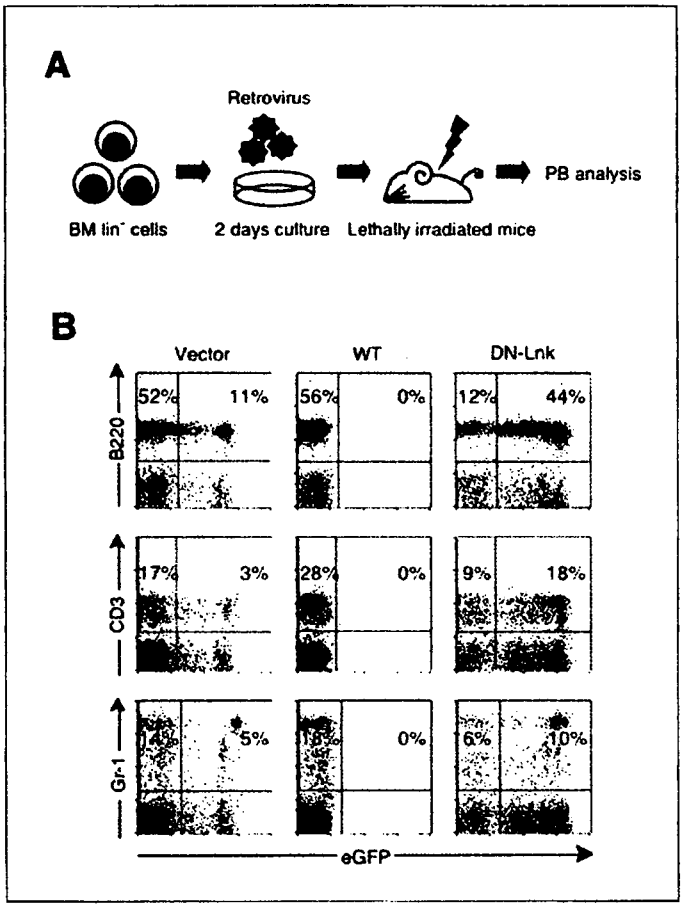

Fig.2 Expression of DN-Lnk in HSC/Ps facilitates blood cell repopulation

(A) Bone marrow transplantation model. Retrovirally transduced Lin⁻ cells were transferred into lethally irradianted mice. Peripheral blood (PB) harvested from transplanted mice was analyzed by flowcytometry.

(B) Contribution of transduced cells to B-, T- and myeloid lineage in PB. Flow cytometric analysis of PB cells from mice 17 weeks after transplantation are shown.

crucial role for inhibiting c-Kit-mediated cell growth and that PH domain and C-terminal tail of Lnk, not Y536 residue within the region, partly contributes to the efficient inhibition.

Screening for dominant negative mutant of Lnk

We next investigated whether non-inhibitory mutants, identified in experiments described above, could exert dominant-negative (DN) effect. Using MC9 transfectant overexpressing Lnk (MC9-Lnk) that hardly proliferates in response to SCF[3], we screened the DN Lnk mutants that could block wild-type Lnk function and cancel the growth inhibition. MC9-Lnk cells expressing R364E outgrew over non-transduced cells, indicating that this mutant acted as a DN mutant. Of generated Lnk mutants, Lnk mutant (dPH/R364E/dC) carrying combined deletion of PH domain and C-terminal tail with R364E mutation exhibited the most strong DN effect (Fig.1). These results suggest that mutation of SH2 domain is critical for DN effect and deletion of PH domain and C-terminal tail supports effective blocking of Lnk function.

Efficient hematopoietic reconstitution by DN Lnk mutant-transduced HSC/Ps in irradiated mice

We next assessed whether dPH/R364E/dC can block the function of Lnk endogenously expressed in HSC/Ps and facilitates the repopulating ability in transplantation model. Lineage marker negative (Lin^-) bone marrow cells containing HSC/Ps was retrovirally transduced with dPH/R364E/dC expression vector for 48 hours and intravenously injected into lethally irradiated recipient mice. Percentage of $eGFP^+$ cells in peripheral blood (PB) cells from the transferred mice was analyzed at several time points after transfer (Fig.2A). Very few $eGFP^+$ cells expressing wild-type Lnk were detected in peripheral lymphocytes, while significant fractions of mature B ($B220^+$)-, T ($CD3^+$)- and myeloid lineage ($Gr\text{-}1^+$) cells were differentiated from $eGFP^+$ cells expressing vector alone. Mice transplanted with DN-Lnk expressing cells displayed significantly higher percentage of $eGFP^+$ cells in each lineage than those transplanted with vector expressing cells (Fig.2B). These results indicated that HSC/Ps expressing DN-Lnk gained enhanced repopulating ability through inhibi-

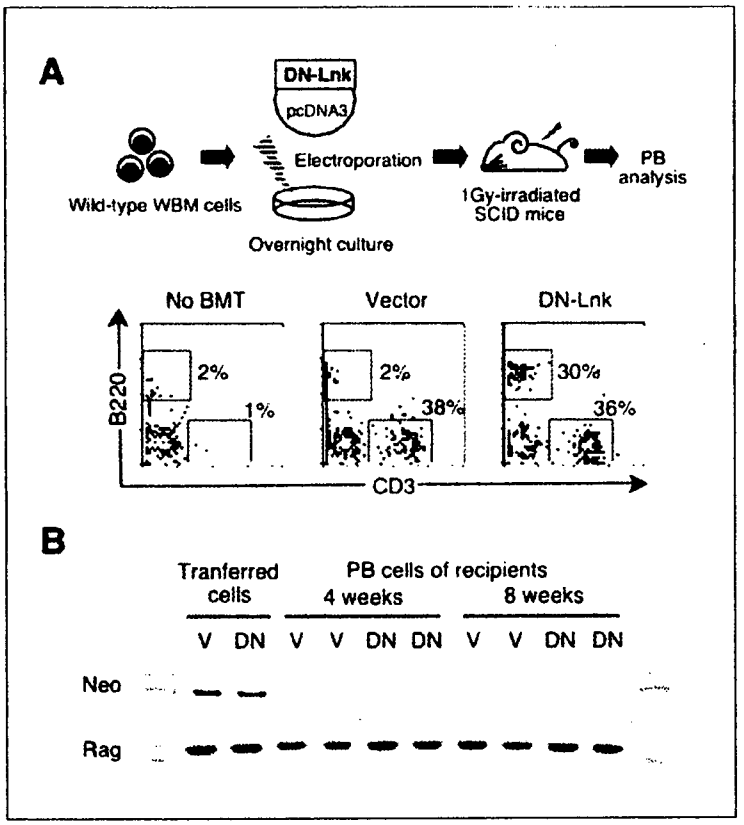

Fig.3 HSC/Ps transiently expressing DN-Lnk also showed efficient reconstitution

(A) Successful reconstitution of lymphoid compartment in SCID mice. Whole bone marrow cells from wild-type mice were transfected with control vector (middle) or DN-Lnk expressing vector (right) and transferred into SCID mice. PB cells obtained from transferred mice were analyzed 8 weeks after transplant.

(B) PCR analysis for plasmid vector in DNA isolated from PB cells of transplanted mice. Probes used are indicated to the left. Genomic DNA content in each sample was normalized by RAG gene. Each lane shows analysis of DNA from individual mouse. V: vector-transfected group, DN: DN-Lnk-transfected group.

tion of Lnk function.

Enhanced engraftment of HSC/Ps by transient inhibition of Lnk

Recent papers have reported that retrovirus-mediated gene transfer into HSC/Ps induces hematologic malignancies because of random integration of transgene into genome of target cells[6,7]. To avoid such side effects accompanied by retroviral transduction, we sought to test the effectiveness of transient expression of DN-Lnk on their engraftment using plasmid vector, which is scarcely integrated into host genome, in competitive repopulation assay. In mice receiving DN-Lnk-transfected HSC/Ps, chimerism of donor-derived cells in all lineage was higher and number of platelets was rapidly recovered compared with control group[8]. We next evaluated the efficacy of transient Lnk inhibition for treatment of severe combined immunodeficient (SCID) mice under nonmyeloablative condition. Bone marrow cells from wild-type animals were transfected with plasmid vector by electroporation, transplanted into SCID mice treated with a low dose of irradiation (1.0 Gly) (Fig.3A). A few control vector-transfected cells engrafted into the BM of recipient animals and gave rise to lymphoid lineage cells. In contrast, DN-Lnk-transfected cells fully reconstituted lymphoid compartment of SCID mice. Especially, rapid and robust production of B-lineage cells was observed from early time point (Fig.3A). Whether the employed plasmid vector was integrated into genome of transfected cells was examined by PCR amplifying neomycin-resistant gene. As expected, neomycin-resistant gene existing only in the plasmid vector was detected in transferred donor cells, however, it was not detected at all in DNA isolated from the reconstituted peripheral blood cells 4 or 8 weeks after transplantation (Fig.3B). These data suggested that transient inhibition of Lnk also could facilitate engraftment of HSC/Ps and early recovery of platelet production with no integration of transgene into genome.

Augmented interaction of HSC/Ps with VCAM-1 by *Lnk* deficiency

The successful multilineage reconstitution by transplanted HSC/Ps requires migration and attachment to a specific microenvironment in bone marrow, so-called niche, where they self-renew and differentiate. Short-term inhibition of Lnk by expressing DN-Lnk enhanced engrafting potential of HSC/Ps. This implies that blocking of Lnk-mediated pathway(s) might affect the migration or adhesion of HSC/Ps to niche shortly after trans-

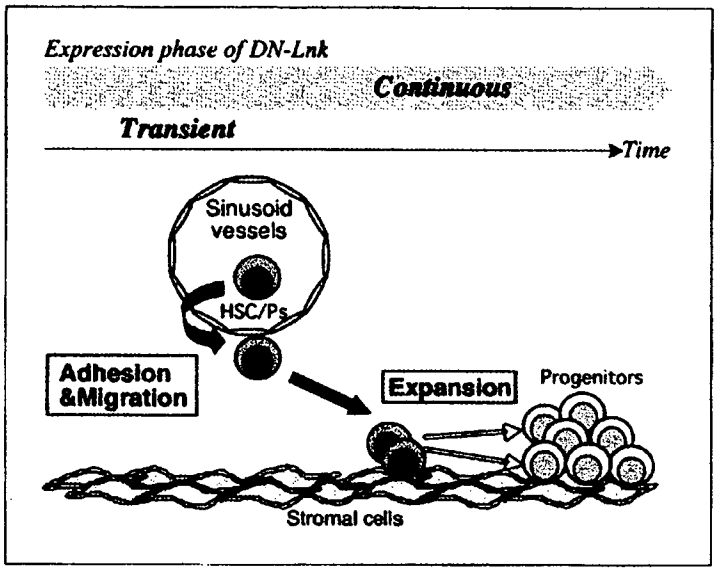

Fig.4 Timing of Lnk inhibition during engraftment of HSC/Ps

plantation in addition to their expansion (Fig.4). To address this possibility, we evaluated the migration responses of Lin⁻ c-Kit⁺ Sca1⁺ cells from *Lnk-/-* or wild-type mice against CXCL12, an essential chemokine for homing of HSC/Ps to BM[9] using transwell migration assay. CXCL12-induced migration through membrane was comparable between *Lnk-/-* and normal progenitors. Interestingly, *Lnk-/-* progenitors didn't migrate as efficiently as wild-type cells in the presence of BM cells other than Lin⁻ cells or VCAM-1, one of extracellular matrices associated with homing of HSC/Ps[8,10]. This implicated that Lnk plays a role in controlling cell motility of HSC/Ps by modulating an interaction between adhesion molecules like VCAM-1 on BM cells and integrins on HSC/Ps.

Perspectives

We identified a dominant-negative mutant of Lnk that blocks Lnk function endogenously expressed on HSC/Ps and established a novel and potential approach to facilitate the engraftment of HSC/Ps by transiently inhibiting Lnk-mediated pathway(s). We showed that retroviral transduction of DN-Lnk can enhance the repopulating capability of HSC/Ps, leading to an increased contribution of transduced cells in lymphoid and myeloid lineage cell production. However, recent studies have reported that retrovirus-mediated transduction into HSC/Ps may lead to unexpected side effects including hamatopoietic disorders or malignant transformations in human and mice due to integration of transgene into the cellular genome and long-term transgene expression[11,12]. Transient expression using plasmid vector has advantage to reduce those side effects because the transgene on plasmid is hardly integrated into cellular genome and declines as transfected cells divide. Short-term expression of DN-Lnk by plasmid vector could successfully augment engrafting potential of HSC/Ps and effectively reconstitute the immune system of immunodeficient animals under non-myeloablative condition. Thus, transient inhibition of Lnk-mediated pathway(s) could provide a useful therapeutic strategy for potentiating HSC/Ps for engraftment without any side effects followed by genetic modification.

We demonstrated that Lnk negatively regulated c-Kit-mediated proliferation and SH2 domain was crucial to the growth inhibition. It has been also shown that Lnk regulates TPO- as well as EPO-dependent growth signals, and the SH2 domain is important[4,13]. Data from transmigration assay indicates that Lnk controls cell motility of HSC/Ps possibly through integrin in addition to their cytokine-dependent expansion (Fig.4). This idea is supported by recent studies regarding APS and SH2-B, the other members of Lnk adaptor family, showing their roles in the regulation of actin cytoskeleton[14-16]. Especially, SH-2B interacts with Rac, small GTP protein, and enhances the growth hormone-induced actin rearrangement and cell motility[14,15]. Rac regulates actin cytoskeleton of HSC/Ps including migration, adhesion and cell cycle progression[17]. Thus, augmented interaction of HSC/Ps with adhesion molecule by blocking Lnk function might increase the chance for transplanted HSC/Ps to lodge in appropriate microenvironment in bone marrow by modulating actin cytoskeleton upon activation via integrins. It is likely that Lnk is a dual-functional adaptor not only controlling the expansion of HSC/Ps through cytokine-dependent pathway, but also modu-

lating their cell motility and/or integrin-mediated responses. The detailed molecular mechanisms by which Lnk modulates cell behavior on adhesion molecules should be addressed in future studies.

Acknowledgements

We would like to thank Drs. Chiyomi Kubo-Akashi, Ikuo Nobuhisa, Sang-Mo Kwon, Masanori Iseki, Toshio Kitamura and Tetsuya Taga for many collaborative works cited in this review. We are also grateful to Drs. Koji Eto, Hideo Ema, Jun Seita and Hiromitsu Nakauchi for helpful discussions. Hitoshi Takizawa is supported by Research Fellowships of the Japan Society for the Promotion of Science for Young Scientists. Our works were supported by Special Coordination Funds for Promoting Science and Technology, Grants-in-Aids from the Ministry of Education, Culture, Sports, Science and Technology, the Japanese Government, and a grant from the Uehara Memorial Foundation.

Reference

1) Morrison SJ, Uchida N, Weissman IL: The biology of hematopoietic stem cells. Annu Rev Cell Dev Biol, 11: 35-71, 1995.
2) Takaki S, Morita H, Tezuka Y, Takatsu K: Enhanced hematopoiesis by hematopoietic progenitor cells lacking intracellular adaptor protein, Lnk. J Exp Med, 195: 151-160, 2002.
3) Ema H, Sudo K, Seita J, Matsubara A, Morita Y, Osawa M, Takatsu K, Takaki S, Nakauchi H: Quantification of self-renewal capacity in single hematopoietic stem cells from normal and Lnk-deficient mice. Dev Cell, 8: 907-914, 2005.
4) Tong W, Lodish HF: Lnk inhibits Tpo-mpl signaling and Tpo-mediated megakaryocytopoiesis. J Exp Med, 200: 569-580, 2004.
5) Buza-Vidas N, Antonchuk J, Qian H, Mansson R, Luc S, Zandi S, Anderson K, Takaki S, Nygren JM, Jensen CT, Jacobsen SE: Cytokines regulate postnatal hematopoietic stem cell expansion: opposing roles of thrombopoietin and LNK. Genes Dev, 20: 2018-2023, 2006.
6) Bunting KD, Galipeau J, Topham D, Benaim E, Sorrentino BP: Transduction of murine bone marrow cells with an MDR1 vector enables ex vivo stem cell expansion, but these expanded grafts cause a myeloproliferative syndrome in transplanted mice. Blood, 92: 2269-2279, 1998.
7) Baum C, Dullmann J, Li Z, Fehse B, Meyer J, Williams DA, von Kalle C: Side effects of retroviral gene transfer into hematopoietic stem cells. Blood, 101: 2099-2114, 2003.
8) Takizawa H, Kubo-Akashi C, Nobuhisa I, Kwon SM, Iseki M, Taga T, Takatsu K, Takaki S: Enhanced engraftment of hematopoietic stem/progenitor cells by the transient inhibition of an adaptor protein, Lnk. Blood, 107: 2968-2975, 2006.
9) Aiuti A, Webb IJ, Bleul C, Springer T, Gutierrez-Ramos JC: The chemokine SDF-1 is a chemoattractant for human CD34+ hematopoietic progenitor cells and provides a new mechanism to explain the mobilization of CD34+ progenitors to peripheral blood. J Exp Med, 185: 111-120, 1997.
10) Papayannopoulou T, Nakamoto B: Peripheralization of hemopoietic progenitors in primates treated with anti-VLA4 integrin. Proc Natl Acad Sci USA, 90: 9374-9378, 1993.
11) Li Z, Dullmann J, Schiedlmeier B, Schmidt M, von Kalle C, Meyer J, Forster M, Stocking C, Wahlers A, Frank O, Ostertag W, Kuhlcke K, Eckert HG, Fehse B, Baum C: Murine leukemia induced by retroviral gene marking. Science, 296: 497, 2002.
12) Hacein-Bey-Abina S, Von Kalle C, Schmidt M, McCormack MP, Wulffraat N, Leboulch P, Lim A, Osborne CS, Pawliuk R, Morillon E, Sorensen R, Forster A, Fraser P, Cohen JI, de Saint Basile G, Alexander I, Wintergerst U, Frebourg T, Aurias A, Stoppa-Lyonnet D, Romana S, Radford-Weiss I, Gross F, Valensi F, Delabesse E, Macintyre E, Sigaux F, Soulier J, Leiva LE, Wissler M, Prinz C, Rabbitts TH, Le Deist F, Fischer A, Cavazzana-Calvo M: LMO2-associated clonal T cell proliferation in two patients after gene therapy for SCID-X1. Science, 302: 415-419, 2003.
13) Tong W, Zhang J, Lodish HF: Lnk inhibits erythropoiesis and Epo-dependent JAK2 activation and downstream signaling pathways. Blood, 105: 4604-4612, 2005.
14) Herrington J, Diakonova M, Rui L, Gunter DR, Carter-Su C: SH2-B is required for growth hormone-induced actin reorganization. J Biol Chem, 275: 13126-13133, 2000.
15) Diakonova M, Gunter DR, Herrington J, Carter-Su C: SH2-Bbeta is a Rac-binding protein that regulates cell motility. J Biol Chem, 277: 10669-10677, 2002.
16) Kubo-Akashi C, Iseki M, Kwon SM, Takizawa H, Takatsu K, Takaki S: Roles of a conserved family of adaptor proteins, Lnk, SH2-B, and APS, for mast cell development, growth, and functions: APS-deficiency causes augmented degranulation and reduced actin assembly. Biochem Biophys Res Commun, 315: 356-362, 2004.
17) Gu Y, Filippi MD, Cancelas JA, Siefring JE, Williams EP, Jasti AC, Harris CE, Lee AW, Prabhakar R, Atkinson SJ, Kwiatkowski DJ, Williams DA: Hematopoietic cell regulation by Rac1 and Rac2 guanosine triphosphatases. Science, 302: 445-449, 2003.

Microbiology (2007), 153, 585–592 DOI 10.1099/mic.0.29213-0

Chlamydial SET domain protein functions as a histone methyltransferase

Masayuki Murata,[1] Yoshinao Azuma,[1] Koshiro Miura,[1,2]† Mohd. Akhlakur Rahman,[1] Minenosuke Matsutani,[1] Masahiro Aoyama,[1] Harumi Suzuki,[1] Kazuro Sugi[2] and Mutsunori Shirai[1]

Correspondence
Yoshinao Azuma
yazuma@yamaguchi-u.ac.jp

Mutsunori Shirai
mshirai@yamaguchi-u.ac.jp

[1]Department of Microbiology and Immunology, Yamaguchi University School of Medicine, 1-1-1 Minami-Kogushi, Ube, Yamaguchi 755-8505, Japan

[2]Department of Clinical Research, National Sanyo Hospital, 685 Higashi-Kiwa, Ube, Yamaguchi 755-0241, Japan

Received 12 June 2006
Revised 20 October 2006
Accepted 20 October 2006

SET domain genes have been identified in numbers of bacterial genomes based on similarity to SET domains of eukaryotic histone methyltransferases. Herein, a *Chlamydophila pneumoniae* SET domain gene was clarified to be coincidently expressed with *hctA* and *hctB* genes encoding chlamydial histone H1-like proteins, Hc1 and Hc2, respectively. The SET domain protein (cpnSET) is localized in chlamydial cells and interacts with Hc1 and Hc2 through the C-terminal SET domain. As expected from conservation of catalytic sites in cpnSET, it functions as a protein methyltransferase to murine histone H3 and Hc1. However, little is known about protein methylation in the molecular pathogenesis of chlamydial infection. cpnSET may play an important role in chlamydial cell maturation due to modification of chlamydial histone H1-like proteins.

INTRODUCTION

Chlamydophila pneumoniae is an obligatory intracellular eubacterium that causes acute respiratory diseases and may be involved in chronic inflammatory processes, such as atherosclerosis (Rosenfeld *et al.*, 2000), asthma (Hahn *et al.*, 1991) and Alzheimer's disease (Itzhaki *et al.*, 2004). Persistence of chlamydial infection has been thought to be important for chronic diseases and has been characterized using model animals and activation stimuli such as cytokines and antibiotics (Beatty *et al.*, 1993; Belland *et al.*, 2003; Malinverni *et al.*, 1995; Mehta *et al.*, 1998). However, molecular-level relationships between chronic disease progression and persistent infection are not yet clear.

Chlamydiae exhibit a unique life cycle in which they alternate morphologies between elementary bodies (EBs) and reticulate bodies (RBs). EBs are transcriptionally inactive electron-dense particles that are internalized into host cells by inducing phagocytosis. EB differentiation into RBs occurs with the development of phagosomes into inclusions. Transcriptionally active RBs multiply by binary fission with nutrients acquired from the host cell. At the end of the developmental cycle, RBs are converted into EBs and released from host cells for the next infection. Besides the developmental cycle, during persistent infection caused by exposure to interferon gamma (IFN-γ) or antibiotics, RBs differentiate into aberrantly large and non-multiplying RBs (Belland *et al.*, 2003). However, little is known about the switching mechanism whereby vegetative RBs convert into infectious EBs or aberrant RBs. Understanding this molecular system should be helpful for the prevention of persistent chlamydial infection.

Two eukaryotic histone H1-like proteins of chlamydiae, Hc1 and Hc2, are present mainly in EBs, where those proteins bind DNA and promote genomic DNA condensation (Barry *et al.*, 1992; Hackstadt *et al.*, 1991; Perara *et al.*, 1992; Tao *et al.*, 1991). Recently a small regulatory RNA gene was identified as a suppressor of the lethal phenotype of *hctA* overexpression in *Escherichia coli* and it was shown to negatively regulate Hc1 synthesis at an early stage of infection (Grieshaber *et al.*, 2006). These histone-like proteins may act as global transcriptional regulators and play a critical role for the transformation of vegetative RBs into infectious EBs. Transcriptional, translational and functional regulations of Hc1 and Hc2 may be important for the morphological switching. Chlamydial genome analyses have revealed the existence of another candidate gene as a regulator of Hc1 and Hc2, termed the *set* gene,

†Present address: Department of Veterinary Biosciences, the Ohio State University, 1900 Coffey Rd, Columbus, OH 43210, USA.

Abbreviations: cpnSET, *Chlamydophila pneumoniae* SET domain protein; EB, elementary body; RB, reticulate body; FCS, fetal calf serum; GST, glutathione *S*-transferase; h.p.i., hours post-infection.

A supplementary table and three supplementary figures are available with the online version of this paper.

which encodes a protein containing a domain similar to the eukaryotic SET domain (Stephens *et al.*, 1998). Eukaryotic SET domains were initially identified in the C-terminal ends of *Drosophila* transcriptional regulatory factors (Alvarez-Venegas & Avramova, 2002; Jones & Gelbart, 1993; Kouzarides, 2002; Kuzmichev *et al.*, 2005) and have been shown to be involved in chromatin remodelling due to histone methyltransferase activity to specific residues in amino-terminal histone tails, such as histone H3 K9 and K27 (Marmorstein, 2003.; Xiao *et al.*, 2003).

Herein, we demonstrate that the chlamydial SET domain protein physically interacts with chlamydial histone-like proteins Hc1 and Hc2, and functions as a histone methyltransferase to methylate mouse histone H3 and Hc1. The results suggest involvement of the SET domain protein in chlamydial cell transformation from RBs to EBs.

METHODS

Chemicals, cell line and bacterial strains. Gentamicin, cycloheximide, Hoechst 33258 and Dulbecco's modified Eagle medium were purchased from Sigma-Aldrich. Fetal calf serum (FCS) was from Cansera International. Anti-*C. pneumoniae*-specific monoclonal antibody (RR402) was purchased from Washington Research Foundation. FITC-conjugated goat anti-mouse antibody and Alexa 545-conjugated goat anti-rabbit antibody were obtained from Invitrogen. *S*-Adenosyl-[methyl-^{14}C]-L-methionine was purchased from Amersham.

HEp-2 cells (ATCC CCL-23) were used as host cells for infection by *C. pneumoniae* J138, isolated in Japan in 1994 (Shirai *et al.*, 2000). *C. pneumoniae* J138 EBs were purified by sucrose-gradient centrifugation and stored at −80 °C in SPG buffer (pH 7.2), which consists of 250 mM sucrose, 10 mM sodium phosphate and 5 mM glutamate. Chlamydial titres were adjusted to 2.0×10^8 inclusion-formation units (i.f.u.) ml^{-1}.

Chlamydial infection. Chlamydial infections were performed by methods described previously (Rahman *et al.*, 2005). Briefly, HEp-2 cells were grown in HEp-2 medium (Dulbecco's modified Eagle medium supplemented with 10 % heat-inactivated FCS and 50 μg gentamicin ml^{-1}) at 37 °C, 5 % CO_2. Prior to infection, 2.0×10^5 HEp-2 cells were seeded to each well of six-well tissue culture plates and allowed to adhere for 24 h. Infection was performed by addition of *C. pneumoniae* J138 EBs at 0.20 m.o.i., followed by centrifugation at 22 °C for 60 min at 700 *g*. After incubation for 30 min at 36 °C, 5 % CO_2, the inocula were replaced with post-infection medium (Dulbecco's modified Eagle medium with 5 % heat-inactivated FCS, 50 μg gentamicin ml^{-1} and 1 μg cycloheximide ml^{-1}). The infectants were incubated for up to 72 h at 36 °C, 5 % CO_2.

Vector construction. pGEX(2T-P)+cpnSET full-length and pGEX(2T-P)+cpnSET (206–219 aa) were constructed by cloning the *C. pneumoniae* J138 *set* gene fragments into pGEX(2T-P) (Azuma *et al.*, 1995). Three deletion series of pGEX(2T-P)+Hc1 [Hc1-1 (aa 1–50), Hc1-2 (aa 41–78) and Hc1-3 (aa 65–123)] were constructed based on the pGEX(2T-P)+Hc1. For the yeast two-hybrid study, pGBKT7+cpnSET was prepared by cloning *C. pneumoniae* J138 *set* gene into pGBKT7 (Clontech). For construction of pGADT7+Hc1 and pGADT7+Hc2, *C. pneumoniae* J138 *hctA* and *hctB* genes, respectively, were cloned into pGADT7 (Clontech). Eight deletion series of pGBKT7-cpnSET were constructed by PCR using pGBKT7-cpnSET. pGEX4T-3-mG9a and pGEX4T-3-H3, encoding GST fusion G9a (621–1000 aa) and GST fusion histone H3 (1–50 aa), respectively, were kind gifts of Professor Yoichi Shinkai (Kyoto University, Kyoto, Japan) (Tachibana *et al.*, 2001). All primers used in this work are shown in Supplementary Table S1, available with the online version of this paper.

Preparation of recombinant proteins and anti-cpnSET antiserum. GST fusion proteins were produced in *E. coli* JM109 cells and purified using glutathione-agarose affinity purification in lysis buffer [20 mM Tris/HCl (pH 8.0), 5 mM EDTA, 0.5 % Triton X-100, 0.2 mM PMSF and a protease inhibitor mixture] (Azuma *et al.*, 1993). One milligram of GST fusion cpnSET protein was cleaved with 0.02 U thrombin (Novagen) in thrombin reaction solution [20 mM Tris/HCl (pH 8.4), 150 mM NaCl, 2.5 mM $CaCl_2$] for 2 h at 20 °C, and the thrombin was removed by incubation with 50 μl *p*-aminobenzamidene-agarose beads (Amersham) for 1 h at 4 °C. Anti-cpnSET rabbit polyclonal sera were prepared by immunization of rabbits five times every other week with 0.1 μg of the purified GST fusion cpnSET (aa 206–219) protein, following the method described previously (Miura *et al.*, 2001).

Histochemical analysis. After fixation with 100 % methanol for 60 min, the infectants were incubated with anti-*C. pneumoniae*-specific monoclonal antibody (RR402) and anti-cpnSET rabbit serum as described above for 60 min at 25 °C. After washing, cells were stained with FITC-conjugated goat anti-mouse antibody and Alexa 545-conjugated goat anti-rabbit antibody. Nucleic acids were stained with 2 μg Hoechst 33258 ml^{-1} for 10 min. Microscopic observation was performed with an LSM510 laser scanning confocal microscope (Zeiss).

Quantitative RT-PCR. For quantitative RT-PCR by a LightCycler (Roche), QuantiTect SYBR Green RT-PCR (Qiagen) was used with a total RNA fraction extracted from *C. pneumoniae*-infected cells. Reactions were performed based on the manufacturer's instructions. All primers are shown as a supplementary table within the online version of this paper at Table S1 for primers.

Protein interaction analyses. Yeast two-hybrid analysis was performed using MatchMaker GAL4 Two-Hybrid System 3 kits (Clontech) according to the manufacturer's instructions. Transformants were assayed by growth on plates without leucine, tryptophan and histidine, and without leucine and tryptophan as a control.

Structure modelling of cpnSET was carried out using the virus SET structure as a template (Eswar *et al.*, 2003; Manzur *et al.*, 2003) and peptide docking analysis onto cpnSET was performed using AutoDock (Morris *et al.*, 1996).

***In vitro* histone methyltransferase assay.** Procedures for *in vitro* measurement of histone methyltransferase activity were adapted from the protocol reported previously (Tachibana *et al.*, 2001). Briefly, the assay was carried out with 0.5 μg mG9a or cpnSET protein and 0.5 μg GST fusion mouse histone H3 or chlamydial Hc1 as a substrate in 50 μl reaction buffer (50 mM Tris/HCl pH 8.5, 20 mM KCl, 10 mM $MgCl_2$, 10 mM β-mercaptoethanol, 250 mM sucrose and 4.6 kBq *S*-adenosyl-[*methyl*-^{14}C]-L-methionine as methyl donor). After incubation for 60 min at 37 °C, reactions were stopped by addition of 15 μl SDS buffer [6 % SDS, 150 mM Tris/HCl (pH 6.8), 300 mM DTT, 0.1 % BPB and 30 % (v/v) glycerol] and boiling at 100 °C for 10 min. Methyl-^{14}C was detected using a BAS-2000 scanner (FujiFilm) after protein separation by 12 % acrylamide SDS-PAGE.

RESULTS

Chlamydial SET domain protein

Chlamydial genome analysis has revealed the existence of a number of genes similar to eukaryotic genes involved in

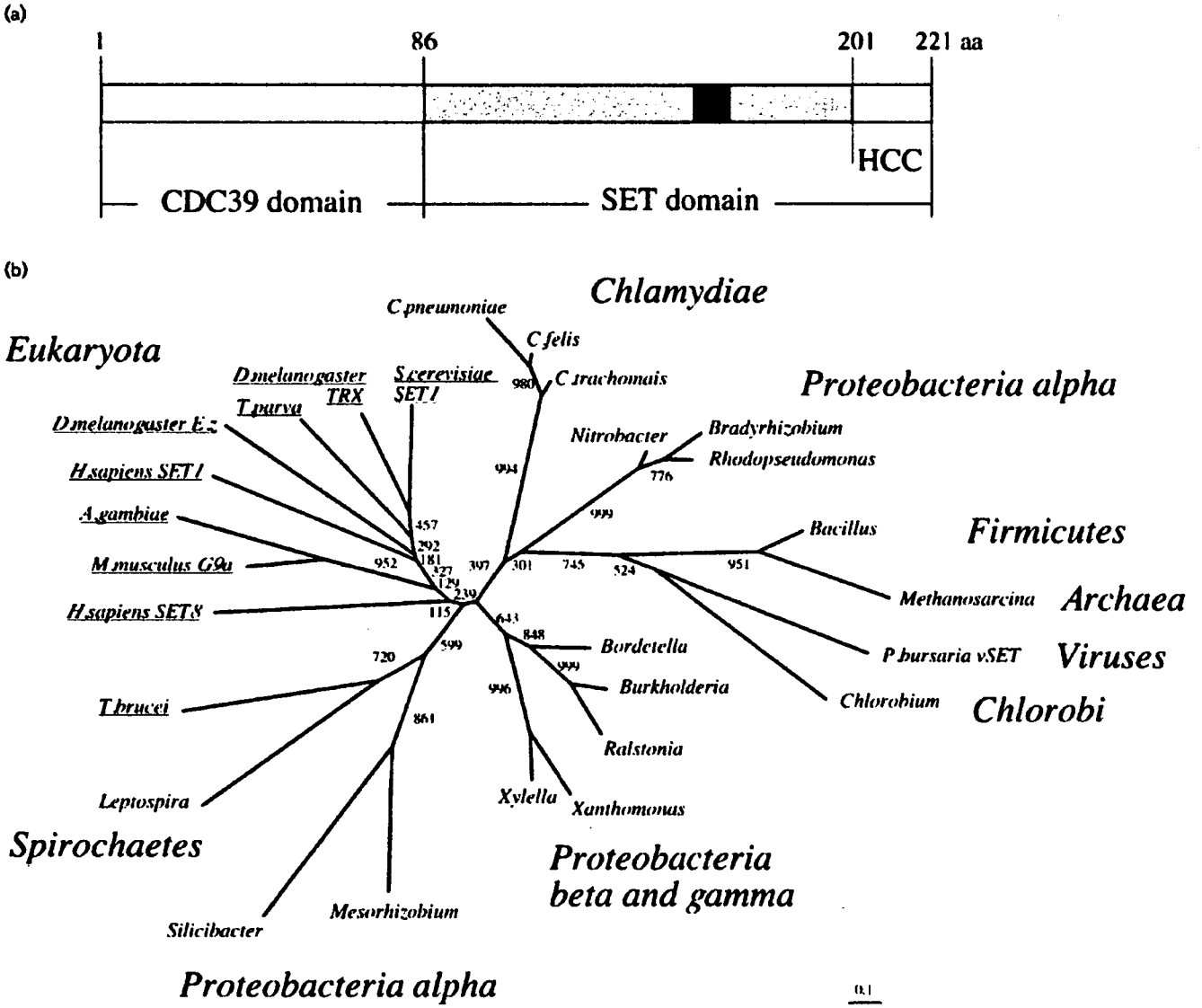

Fig. 1. *C. pneumoniae* SET domain protein (cpnSET). (a) Domains in cpnSET domain protein. The signature motif, 'RFINHXCXPN' (Dillon *et al.*, 2005) is indicated with a black box. The HCC in the C-terminus shows a highly charged and conserved (HCC) domain. (b) Phylogenetic analysis of SET-domain proteins based on sequence alignment. The alignment includes the known members of the SET-domain protein family. *C. pneumoniae*, *Chlamydophila pneumoniae* J138 (NP300935); *C. felis*, *Chlamydophila felis* Fe/C-56 (CF0125); *C. trachomatis*, *Chlamydia trachomatis* D/UW-3/CX (NP220256); *Bradyrhizobium*, *Bradyrhizobium japonicum* USDA110 (BAC51052); *Rhodopseudomonas*, *Rhodopseudomonas palustris* BisA53 (ZP00807683); *Nitrobacter*, *Nitrobacter winogradskyi* Nb-255 (ABA05415); *Bacillus*, *Bacillus anthracis* Ames (ZP00390019); *Burkholderia*, *Burkholderia cenocepacia* (ZP00459508); *Ralstonia*, *Ralstonia eutropha* JMP134 (AAZ62749); *Bordetella*, *Bordetella pertussis* 12822 (CAE44800); *Xanthomonas*, *Xanthomonas oryzae* MAFF (YP200046); *Xylella*, *Xylella fastidiosa* (AAF84287); *Mesorhizobium*, *Mesorhizobium loti* MAFF303099 (BAB50081); *Silicibacter*, *Silicibacter pomeroyi* DSS-3 (AAV95586); *Chlorobium*, *Chlorobium tepidum* TLS (AAM72187); *Leptospira*, *Leptospira interrogans* serovar Copenhageni str. (AAS71524); *Methanosarcina*, *Methanosarcina mazei* Go1 (AAM32541); *P. bursaria* vSET, *Paramecium bursaria chlorella* virus-1 (NP048968); *H. sapiens* SET1, *Homo sapiens* (NP071900); *H. sapiens* SET8, *Homo sapiens* (NP065115); *M. musculus* G9a, *Mus musculus* (NP665829); *D. melanogaster* TRX, *Drosophila melanogaster* (NP599109); *D. melanogaster* E.z., *Drosophila melanogaster* (AAF50149); *S. cerevisiae* SET1, *Saccharomyces cerevisiae* S288C (P38827); *T. parva*, *Theileria parva* Muguga (AN32159); *T. brucei*, *Trypanosoma brucei* TREU927/4 (EAN77879); *A. gambiae*, *Anopheles gambiae* PEST (EAA07914).

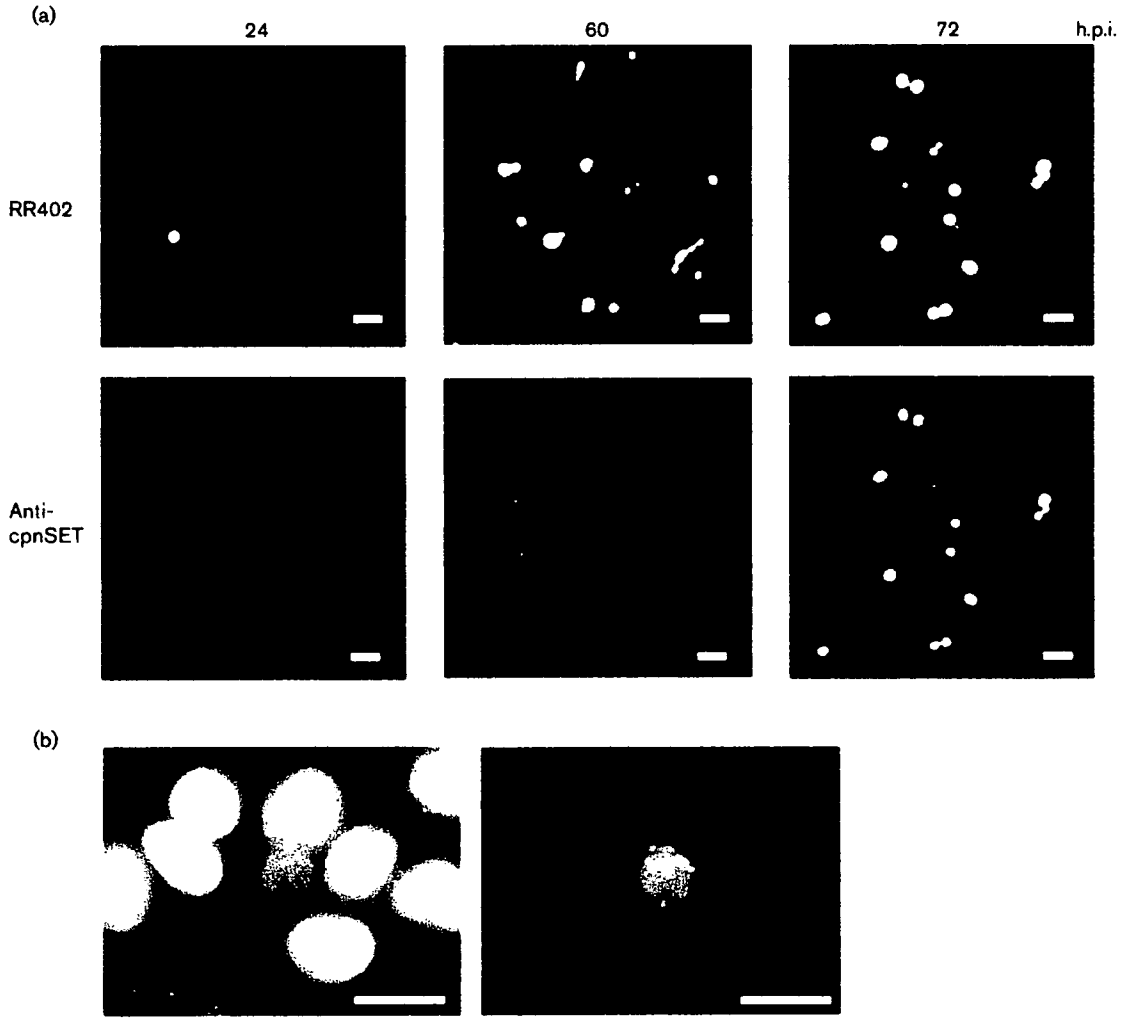

Fig. 2. Expression and localization of cpnSET within *C. pneumoniae* J138-infected HEp-2 cells. (a) Infected cells were fixed at 24, 60 and 72 h.p.i. and stained with the indicated antibodies. The anti-cpnSET is *C. pneumoniae* SET-specific rabbit polyclonal antibody prepared in this work and RR402 is *C. pneumoniae*-specific murine monoclonal antibody used as a control. Magnification, ×400; bars, 10 μm. (b) The left and right panels are Hoechst 33258 and anti-cpnSET rabbit serum staining, respectively. Magnification, ×1000; bars, 5 μm.

chromatin maintenance, such as histone, SET and SWI/SNF (Azuma *et al.*, 2006; Carlson *et al.*, 2005; Kalman *et al.*, 1999; Read *et al.*, 2000, 2003; Shirai *et al.*, 2000; Stephens *et al.*, 1998; Thomson *et al.*, 2005). CPj0878 is assigned as a gene coding a SET domain protein in *C. pneumoniae* J138 and well conserved (overall more than 60% identities) in the family *Chlamydiaceae*. The C-terminal SET domain shows approximately 30% identities to many eukaryotic SET domains. The eukaryotic SET domains are well characterized as catalytic domains of histone methyltransferases involved in chromatin remodelling, especially transcriptional regulation and establishment of heterochromatin (Marmorstein, 2003.; Xiao *et al.*, 2003). The chlamydial SET domain protein consists of two distinct domains, CDC39 and SET (Fig. 1a). The N-terminal one-third is partially similar to a CDC39/*Not*I component in a yeast general transcription-negative regulator CCR4–Not complex involved in controlling mRNA initiation (Liu *et al.*, 1998). This CDC39 region is well conserved only in chlamydial SET domain proteins but not in other organism SET proteins. The C-terminal two-thirds region preserves SET signature motifs, such as *S*-adenosyl-L-methionine-binding sites and a catalytic site for the histone methyltransferase activity (Zhang *et al.*, 2003).

The chlamydial SET domain gene (*set*) was thought to be established as a result of horizontal gene transfer from a eukaryotic organism to a chlamydial ancestor (Stephens *et al.*, 1998). But recent progress in genome analysis has revealed the existence of numbers of genes encoding SET-like domains in non-eukaryotic organisms, e.g. *Paramecium bursaria chlorella* virus-1 (Manzur *et al.*, 2003), archaeal

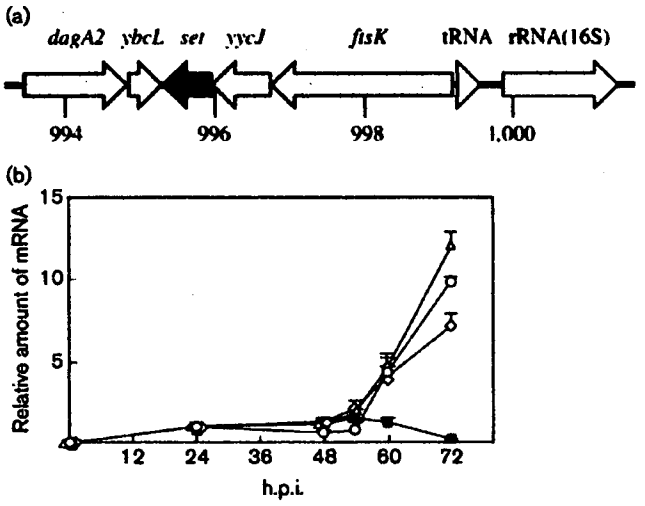

Fig. 3. *C. pneumoniae set* gene. (a) Genome map showing the *set* gene locus. (b) Quantitative RT-PCR of *set*, *hctA*, *hctB* and *ompA* genes. Total RNA was prepared from HEp-2 cells (ATCC CCL-23) infected with *C. pneumoniae* J138 (Rahman *et al.*, 2005) at 0, 12, 24, 48, 54, 60 and 72 h.p.i. Infection was carried out as described previously (Rahman *et al.*, 2005). Expression of *set* (○), *hctA* (△), *hctB* (◇) and *ompA* (■) genes were normalized with 16S rRNA. Relative expression was calculated as the ratio to the value of the expression of each gene at 24 h.

Methanosarcina mezei (Manzur & Zhou, 2005) and a variety of eubacterial phyla such as *Firmicutes*, *Proteobacteria*, *Chlorobi*, *Spirochaetes* and *Chlamydiae*. Phylogenetic analysis of eubacterial and other SETs illustrates that eubacterial SETs diverge into a few groups similar to the general taxological phyla (Fig. 1b). It suggests that chlamydial *set* genes are not transferred horizontally from eukaryotic organisms, but rather likely diverged from a bacterial origin. The sequence alignment of SETs is shown as Supplementary Fig. S1 with the online version of this paper.

Gene expression and protein localization of cpnSET

Since the existence of the *C. pneumoniae* SET domain protein (cpnSET) was proposed based on prediction by genomic analysis, prior to functional analyses, its gene expression and protein localization were investigated by quantitative RT-PCR and immunohistochemical observation. Anti-cpnSET rabbit polyclonal serum prepared in this work was used to detect cpnSET protein in HEp-2 cells infected with *C. pneumoniae* J138. Simultaneously, anti-*C. pneumoniae*-specific monoclonal antibody RR402 and Hoechst 33258 were used for counter-staining. While chlamydial inclusions visualized by RR402 were detectable at any stages, cpnSET was detected only at 60 and 72 h post-infection (h.p.i.) (Fig. 2a) and in chlamydial cells (Fig. 2b). It is a similar expression pattern of Hc1 and Hc2 proteins encoded by *hctA* and *hctB* genes, respectively (Hackstadt *et al.*, 1991).

In chlamydial genomes, *ftsK*, *yycJ* and *set* genes are closely located in this order and seem to constitute an operon (Fig. 3a). In contrast to SET protein accumulation (Fig. 2a), chlamydial *ftsK* has been shown to express constantly from middle to late infection stages (Byrne *et al.*, 2001) and our data from microarray analyses for chlamydial expression showed results consistent with this (data not shown). To clarify the expression of *set*, quantitative RT-PCR was performed. Relative expression of *set*, *ompA*, *hctA* and *hctB* normalized to 16S rRNA amount are shown in Fig. 3(b). Constant expression of *ompA* and late-stage expression of *hctA* and *hctB* were consistent with previous reports (Fahr *et al.*, 1995; Slepenkin *et al.*, 2003). The accumulation of *set* mRNA was increased simultaneously with *hctA* and *hctB* after 54 h.p.i., suggesting that *set* may be transcriptionally independent of *ftsK* and regulated in the same manner as *hctA* and/or *hctB*.

CpnSET interaction with histone-like protein

Physical interaction of cpnSET with Hc1 and Hc2 was tested by the yeast two-hybrid system. It was clarified that cpnSET can interact with Hc1 and Hc2. Based on the experiments using deletion series of cpnSET, the binding to the Hc1 and Hc2 is through aa 137–200 and 137–160, respectively, of cpnSET, both of which regions contain substrate-binding amino acids required for histone methyltransferase activity (Fig. 4a). SET protein localization, expression stage and interaction with Hc1 and Hc2 strongly suggest that cpnSET catalyses protein methylation to Hc1 and Hc2 proteins. The original data for the yeast two-hybrid system are shown as Supplementary Fig. S2 with the online version of this paper.

To know whether cpnSET functions as a methyltransferase, an *in vitro* methyltransferase assay was carried out using recombinant murine histone H3 as a substrate under the conditions optimized for mouse G9a, which is a major mammalian histone methyltransferase containing a SET domain responsible for methylation of K9 in histone H3 at euchromatin (Tachibana *et al.*, 2001). A 0.5 μg sample of cpnSET, GST and G9a proteins was separately incubated with 0.5 μg recombinant mouse histone H3. It was shown that cpnSET can methylate histone H3 and the methylation activity of cpnSET is 14% of G9a under these conditions (Fig. 4b).

As a substrate candidate of chlamydial proteins for cpnSET activity, Hc1 protein was subjected to this assay with Hc1-1, Hc1-2 and Hc1-3 (aa 1–50, 41–78 and 65–123, respectively). The full lengths of Hc1 and Hc2 are difficult to keep soluble in the processes of protein purification and methyltransferase reaction. As a result, only the Hc1-1 was capable of being methylated by cpnSET (Fig. 4c). No apparently conserved sequences were found between H3 (aa 1–50) and Hc1-1 (Fig. 4c). However, the combination of two informatics analyses, structure modelling of cpnSET using the virus SET

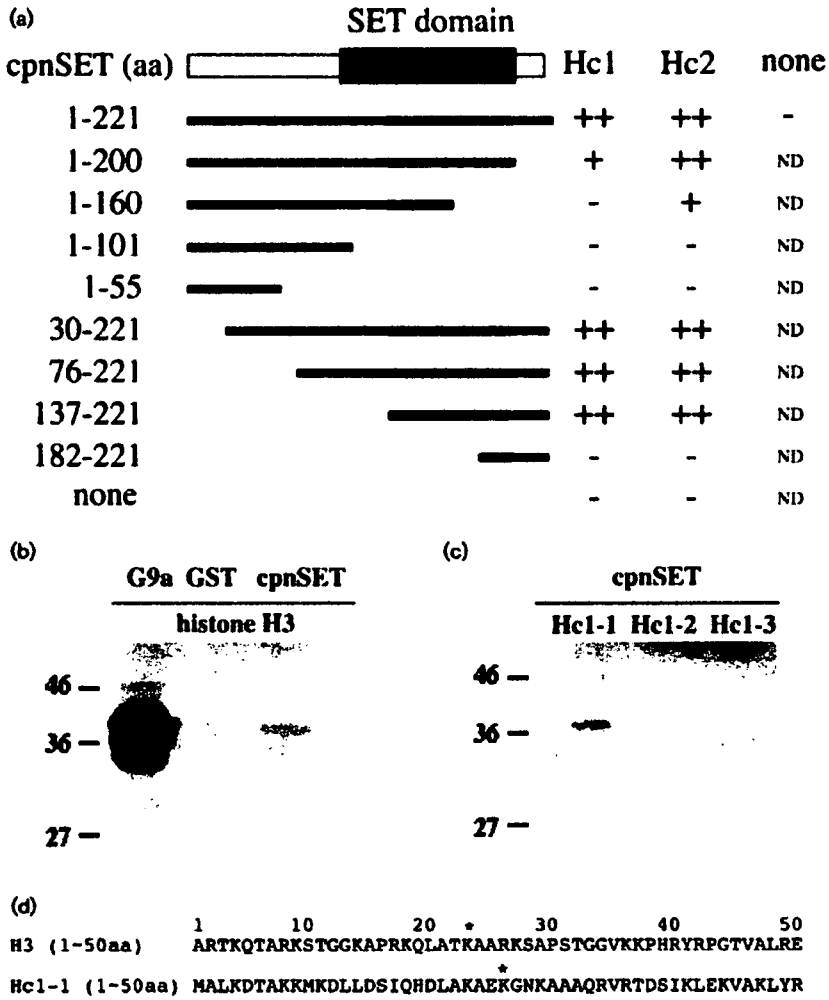

Fig. 4. Interaction of cpnSET and chlamydial histone-like proteins. (a) Two-hybrid assay between cpnSET or its deletion series, and Hc1 and Hc2. The filled box (aa 102–181) and grey region show the SET domain and interaction domain of cpnSET with Hc1 and Hc2, respectively. ++, + and −, good, weak, and no growth, respectively, on culture medium without histidine. None, vector only; ND, not determined. (b) Histone H3 methylation. GST-G9a (indicated as G9a), GST-cpnSET (cpnSET) and GST protein (GST) were subjected to methylation of GST-H3 protein (histone H3). (c) Chlamydial Hc1 methylation. Hc1 deletion proteins Hc1-1, Hc1-2 and Hc1-3 were used as substrates for *in vitro* methylation by chlamydial GST-cpnSET (cpnSET). (d) Alignments of histone H3 and chlamydial histone-like protein, Hc1-1. Histone H3 (CAH73371) and Hc1-1 (NP_300943) are shown 50 aa from the N terminus. The predicted methylated residues are indicated with asterisks.

structure and peptide docking analysis, indicates that K27 of H3, one of the specific methylation sites (Tachibana *et al.*, 2001), and K29 of Hc1 were the best-fitting lysine residues to the catalytic space of cpnSET on the basis of the lowest docking energy. The modelled cpnSET structure and docking profile are shown in Supplementary Fig. S3 with the online version of this paper.

DISCUSSION

Numbers of genes encoding SET domain proteins have been identified in genomes of non-eukaryotic organisms, e.g. *Paramecium bursaria chlorella* virus-1, archaeal *Methanosarcina mezei* and bacterial *Bacillus anthracis*, *Bacillus cereus*, *Xylella fastidiosa*, *Leptospira interrogans*, *Bradyrhizobium japonicum*, *Chlorobium tepidum* and species of the family *Chlamydiaceae*. It has been reported that the viral SET domain protein methylates histone H3 Lys27, and the archaeal SET domain protein methylates lysine residues of eukaryotic histone H4 and archaeal DNA-binding protein MC1-α (Manzur *et al.*, 2003; Manzur & Zhou, 2005). Herein, cpnSET was shown to function as a protein methyltransferase to methylate both murine histone H3 and chlamydial Hc1 *in vitro*, suggesting that cpnSET may play an important role in modification of Hc1 proteins for the morphological change from RBs to EBs. Since localization of cpnSET was shown mainly in chlamydial cells, cpnSET may methylate Hc1 *in vivo*, but it is still possible that chlamydial SET proteins are exported into host cells or that host histones are transported into chlamydial cells, and then cpnSET and host histones functionally interact with each other. Identification of physiological substrates for methylation by cpnSET and, if Hc1 is one of the physiological substrates for methylation *in vivo*, elucidation of the significance of Hc1 protein modification remains for further investigation. Here one of the eubacterial SET domain proteins was revealed as a protein methyltransferase, and this finding suggests that other eubacterial SET domain proteins may function as methyltransferases as well.

ACKNOWLEDGEMENTS

We thank Dr Yoichi Shinkai and Dr Makoto Tachibana for giving us plasmids (G9a, H3) and Mr Michael S. Patrick for help. This study was supported by Basic and Applied Research on Microbial Genome and

Physiology, a Grant-in-Aid for Scientific Research (KAKEN-HI: 14770063, 16790225) and the National Project on Protein Structural and Functional Analyses from the Ministry of Education, Culture, Sports, Science and Technology of Japan.

REFERENCES

Alvarez-Venegas, R. & Avramova, Z. (2002). SET-domain proteins of the Su(var)3-9, E(z) and Trithorax families. *Gene* **285**, 25–37.

Azuma, Y., Yamagishi, M. & Ishihama, A. (1993). Subunits of the *Schizosaccharomyces pombe* RNA polymerase II: enzyme purification and structure of the subunit 3 gene. *Nucleic Acids Res* **21**, 3749–3754.

Azuma, Y., Tabb, M. M., Vu, L. & Nomura, M. (1995). Isolation of a yeast protein kinase that is activated by the protein encoded by *SRP1* (Srp1p) and phosphorylates Srp1p complexed with nuclear localization signal peptides. *Proc Natl Acad Sci U S A* **92**, 5159–5163.

Azuma, Y., Hirakawa, H., Yamashita, A., Cai, Y., Rahman, M. A., Suzuki, H., Mitaku, S., Toh, H., Goto, S. & other authors (2006). Genome sequence of the cat pathogen, *Chlamydophila felis*. *DNA Res* **13**, 15–23.

Barry, C. E., Hayes, S. F. & Hackstadt, T. (1992). Nucleoid condensation in *Escherichia coli* that express a chlamydial histone homolog. *Science* **256**, 377–379.

Beatty, W. L., Byrne, G. I. & Morrison, R. P. (1993). Morphologic and antigenic characterization of interferon gamma-mediated persistent *Chlamydia trachomatis* infection in vitro. *Proc Natl Acad Sci U S A* **90**, 3998–4002.

Belland, R. J., Nelson, D. E., Virok, D., Crane, D. D., Hogan, D., Sturdevant, D., Beatty, W. L. & Caldwell, H. D. (2003). Transcriptome analysis of chlamydial growth during IFN-gamma-mediated persistence and reactivation. *Proc Natl Acad Sci U S A* **100**, 15971–15976.

Byrne, G. I., Ouellette, S. P., Wang, Z., Rao, J. P., Lu, L., Beatty, W. L. & Hudson, A. P. (2001). *Chlamydia pneumoniae* expresses genes required for DNA replication but not cytokinesis during persistent infection of HEp-2 cells. *Infect Immun* **69**, 5423–5429.

Carlson, J. H., Porcella, S. F., McClarty, G. & Caldwell, H. D. (2005). Comparative genomic analysis of *Chlamydia trachomatis* oculotropic and genitotropic strains. *Infect Immun* **73**, 6407–6418.

Dillon, S. C., Zhang, X., Trievel, R. C. & Cheng, X. (2005). The SET-domain protein superfamily: protein lysine methyltransferases. *Genome Biol* **6**, 227.

Eswar, N., John, B., Mirkovic, N., Fiser, A., Ilyin, V. A., Pieper, U., Stuart, A. C., Marti-Renom, M. A., Madhusudhan, M. S. & other authors (2003). Tools for comparative protein structure modeling and analysis. *Nucleic Acids Res* **31**, 3375–3380.

Fahr, M. J., Douglas, A. L., Xia, W. & Hatch, T. P. (1995). Characterization of late gene promoters of *Chlamydia trachomatis*. *J Bacteriol* **177**, 4252–4260.

Grieshaber, N. A., Grieshaber, S. S., Fischer, E. R. & Hackstadt, T. (2006). A small RNA inhibits translation of the histone-like protein Hc1 in *Chlamydia trachomatis*. *Mol Microbiol* **59**, 541–550.

Hackstadt, T., Baehr, W. & Ying, Y. (1991). *Chlamydia trachomatis* developmentally regulated protein is homologous to eukaryotic histone H1. *Proc Natl Acad Sci U S A* **88**, 3937–3941.

Hahn, D. L., Dodge, R. W. & Golubjatnikov, R. (1991). Association of *Chlamydia pneumoniae* (strain TWAR) infection with wheezing, asthmatic bronchitis, and adult-onset asthma. *JAMA* **266**, 225–230.

Itzhaki, R. F., Wozniak, M. A., Appelt, D. M. & Balin, B. J. (2004). Infiltration of the brain by pathogens causes Alzheimer's disease. *Neurobiol Aging* **25**, 619–627.

Jones, S. R. & Gelbart, W. M. (1993). The drosophila polycomb-group gene enhancer of zeste contains a region with sequence similarity to trithorax. *Mol Cell Biol* **13**, 6357–6366.

Kalman, S., Mitchell, W., Marathe, R., Lammel, C., Fan, J., Hyman, R. W., Olinger, L., Grimwood, J., Davis, R. W. & Stephens, R. S. (1999). Comparative genomes of *Chlamydia pneumoniae* and *C. trachomatis*. *Nat Genet* **21**, 385–389.

Kouzarides, T. (2002). Histone methylation in transcriptional control. *Curr Opin Genet Dev* **12**, 198–209.

Kuzmichev, A., Margueron, R., Vaquero, A., Preissner, T. S., Scher, M., Kirmizis, A., Ouyang, X., Brockdorff, N., Abate-Shen, C. & other authors (2005). Composition and histone substrate of polycomb repressive group complexes change during cellular differentiation. *Proc Natl Acad Sci U S A* **102**, 1859–1864.

Liu, H. Y., Badarinarayana, V., Audino, D. C., Rappsilber, J., Mann, M. & Denis, C. L. (1998). The NOT proteins are part of the CCR4 transcriptional complex and affect gene expression both positively and negatively. *EMBO J* **17**, 1096–1106.

Malinverni, R., Kuo, C. C., Campbell, L. A. & Grayston, J. T. (1995). Reactivation of *Chlamydia pneumoniae* lung infection in mice by cortisone. *J Infect Dis* **172**, 593–594.

Manzur, K. L. & Zhou, M. M. (2005). An archaeal SET domain protein exhibits distinct lysine methyltransferase activity towards DNA-associated protein MC1-alpha. *FEBS Let* **579**, 3859–3865.

Manzur, K. L., Farooq, A., Zeng, L., Plotnikova, O., Koch, A. W., Sachchidanand & Zhou, M. M. (2003). A dimeric viral SET domain methyltransferase specific to Lys27 of histone H3. *Nat Struct Biol* **10**, 187–196.

Marmorstein, R. (2003). Structure of SET domain proteins: a new twist on histone methylation. *Trends Biochem Sci* **28**, 59–62.

Mehta, S. J., Miller, R. D., Ramirez, J. A. & Summersgill, J. T. (1998). Inhibition of *Chlamydia pneumoniae* replication in HEp-2 cells by interferon-gamma: role of tryptophan catabolism. *J Infect Dis* **177**, 1326–1331.

Miura, K., Inouye, S., Sakai, K., Takaoka, H., Kishi, F., Tabuchi, M., Tanaka, T., Matsumoto, H., Shirai, M. & other authors (2001). Cloning and characterization of adenylate kinase from *Chlamydia pneumoniae*. *J Biol Chem* **276**, 13490–13498.

Morris, G. M., Goodsell, D. S., Huey, R. & Olson, A. J. (1996). Distributed automated docking of flexible ligands to proteins: parallel applications of AutoDock 2.4. *J Comput Aided Mol Des* **10**, 293–304.

Perara, E., Ganem, D. & Engel, J. N. (1992). A developmentally regulated chlamydial gene with apparent homology to eukaryotic histone H1. *Proc Natl Acad Sci U S A* **89**, 2125–2129.

Rahman, M. A., Azuma, Y., Fukunaga, H., Murakami, T., Sugi, K., Fukushi, H., Miura, K., Suzuki, H. & Shirai, M. (2005). Serotonin and melatonin, neurohormones for homeostasis, as novel inhibitors of infections by the intracellular parasite *Chlamydia*. *J Antimicrob Chemother* **56**, 861–868.

Read, T. D., Brunham, R. C., Shen, C., Gill, S. R., Heidelberg, J. F., White, O., Hickey, E. K., Peterson, J., Utterback, T. & other authors (2000). Genome sequences of *Chlamydia trachomatis* MoPn and *Chlamydia pneumoniae* AR39. *Nucleic Acids Res* **28**, 1397–1406.

Read, T. D., Myers, G. S. A., Brunham, R. C., Nelson, W. C., Paulsen, I. T., Heidelberg, J., Holtzapple, E., Khouri, H., Federova, N. B. & other authors (2003). Genome sequence of *Chlamydophila caviae* (*Chlamydia psittaci* GPIC): examining the role of niche-specific genes in the evolution of the *Chlamydiaceae*. *Nucleic Acids Res* **31**, 2134–2147.

Rosenfeld, M. E., Blessing, E., Lin, T. M., Moazed, T. C., Campbell, L. A. & Kuo, C. (2000). *Chlamydia*, inflammation, and atherogenesis. *J Infect Dis* **181 Suppl 3**, S492–S497.